Drug Design, Development and Therapy

Dovepress
Taylor & Francis Group

Open Access Full Text Article

ORIGINAL RESEARCH

Unveiling the Therapeutic Potential of Banxia Xiexin Decoction in Alzheimer's Disease: Insights From Network Pharmacology and Experimental Validation

Gaofeng Qin[1–3,*], Rongqiang Song[1,*], Jingyi Sun[4], Juanjuan Dai[3], Wentao Wang[3], Fantao Meng[3], Dan Wang[3], Zhe Liu[1], Baoliang Sun[5], Chen Li[3]

[1]Department of Traditional Chinese Medicine, Binzhou Medical University Hospital, Binzhou, Shandong, People's Republic of China; [2]Postdoctoral Research Mobile Station, Shandong University of Traditional Chinese Medicine, Jinan, Shandong, People's Republic of China; [3]Medical Research Center, Binzhou Medical University Hospital, Binzhou, Shandong, People's Republic of China; [4]Shandong Provincial Hospital Affiliated to Shandong First Medical University, Jinan, Shandong, People's Republic of China; [5]Second AfFIliated Hospital, Shandong First Medical University & Shandong Academy of Medical Sciences, Taian, Shandong, People's Republic of China

*These authors contributed equally to this work

Baoliang Sun, Shandong Provincial Hospital Affiliated to Shandong First Medical University, Jinan, Shandong, People's Republic of China, Email blsun@sdfmu.edu.cn; Chen Li, Medical Research Center, Binzhou Medical University Hospital, Binzhou, Shandong, People's Republic of China, Email lc_0625@163.com

Background: Alzheimer's disease (AD) is associated with various pathological states for which there is no effective treatment. First documented in the Eastern Han Dynasty's medical classic, "Treatise on Febrile and Miscellaneous Diseases" (200–210 Anno Domini), Banxia Xiexin Decoction (BXD) stands as a quintessential approach to treating spleen ailments. Recent studies have shown BXD's effectiveness in mitigating memory impairment associated with AD. Yet, the precise mechanisms underlying BXD's action against AD require further exploration.

Aim of the Study: To explore the important components of BXD in exerting anti-AD effects and the underlying molecular mechanisms using network pharmacology, metabolomics analysis, and in vitro and in vivo validation strategies. Initially, candidates for BXD's application in AD therapy were identified through extensive database searches, followed by an analysis of protein-protein interactions (PPI). To elucidate BXD's therapeutic pathways in AD, we engaged in Gene Ontology (GO) enrichment and Kyoto Encyclopedia of Genes and Genomes (KEGG) assessments. Further, we delved into BXD's primary constituents through ultra-high-pressure liquid chromatography coupled with Q Exactive mass spectrometry and molecular docking techniques. Finally, AD-associated $A\beta_{42}$-SY5Y cells and APPswe/PS1dE9 (APP/PS1) transgenic mice models were utilized to further determine the activity and mechanisms of BXD through various molecular or phenotypic assays and metabolomics analysis.

Results: Our findings identified the PI3K/Akt signaling pathways as central to BXD's effects. Using in vitro and in vivo models, we found the activity of BXD against AD to be mediated by the suppression of neuroinflammation and apoptosis, accompanied by activation of the PI3K/Akt pathway. Finally, we observed robust changes in metabolite levels in the plasma of BXD-treated APP/PS1 mice.

Conclusion: Through systematic data analysis and experimental validation, the therapeutic advantages and fundamental molecular mechanisms of BXD in treating AD were revealed. These findings underscore the promising prospects and compelling potential of BXD, which targets the PI3K/Akt signaling pathway and inflammation, apoptosis, as a therapeutic strategy for improving AD.

Keywords: banxia xiexin decoction, Alzheimer's disease, network pharmacology, apoptosis, neuroinflammation, metabolomics

Received: 23 October 2024
Accepted: 13 March 2025
Published: 21 March 2025

Graphical Abstract

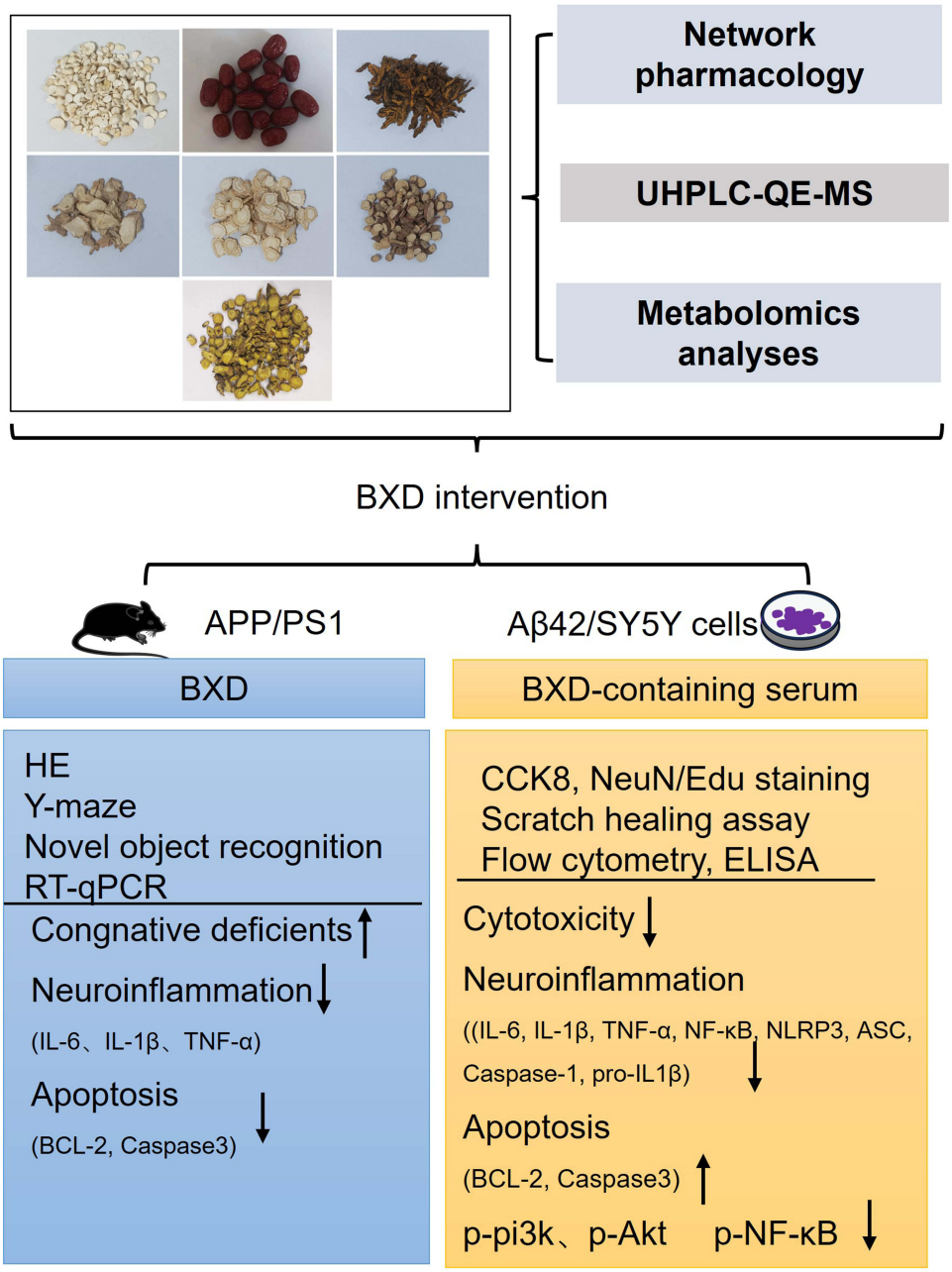

Introduction

Alzheimer's Disease (AD), a prevalent neurodegenerative ailment, primarily exhibits alterations in behavior, impairments in memory, and disruptions in visuospatial abilities, significantly impacting patients' standard of living.[1] According to relevant survey data, it is estimated that there will be approximately 66 million patients with AD worldwide by 2030, and the prevention and treatment of AD is a global problem that needs to be solved urgently[2] The "Alzheimer's Disease Report in China 2024" indicates that in 2021, the number of existing cases of AD and other dementias in China reached 16.99 million, with a prevalence rate of 119.42 per 100,000 population and a mortality rate of 34.6 per 100,000 population, among which the incidence rate in females is higher than in males.[3] The core pathological markers of AD

are β-amyloid (Aβ) plaque and neurofibrillary tangles.[4] Currently, widely recognized hypotheses include the amyloid cascade hypothesis, abnormal tau phosphorylation hypothesis, and cholinergic hypothesis.[5] Treatments for AD include cholinesterase inhibitors (galantamine, donepezil, and cabalatine) and N-methyl-D-aspartic acid receptor antagonists (memantine).[6] Although these drugs can partially alleviate the behavioral and cognitive impairments in patients with AD, their therapeutic effects remain limited.[5] Therefore, therapeutic drugs and methods for the treatment of AD require further investigation.

In recent years, traditional Chinese medicinal (TCM) herbs have been the focus of attention and have been used for their wide range of pharmacological activities and better protective effects against AD.[7] First documented in the Eastern Han Dynasty's medical classic, "Treatise on Febrile and Miscellaneous Diseases" (200–210 Anno Domini), Banxia Xiexin Decoction (BXD) stands as a quintessential approach to treating spleen ailments. From the classic text 《HuangdiNeijing》, it is stated: "That which the heart recalls is called 'yi' (intention), and that which 'yi' holds is called 'zhi' (will)." The five viscera house the spirit, with the spleen housing 'yi' and the kidney housing 'zhi'. The theoretical basis for the treatment of dementia with BXD can be explored from the perspective of regulating the spleen's function of housing 'yi'. That is, the root of the kidney's failure to house 'zhi' lies in the spleen's inability to house 'yi'. Our previous research has demonstrated that BXD exerts a beneficial effect on improving insulin signaling pathways and regulating the gut microbiome, which alleviates the brain glucose metabolism disorder in APP/PS1 mice, thereby enhancing cognition.[8,9] Other studies have shown that the main components of BXD, such as guanyl, ginsenosides, berberine, and liquiritin, alleviate learning and memory deficits and cellular toxicity in AD-related models in vivo and in vitro by affecting multiple pathways or molecular functions, including autophagy and ferroptosis, and the activities of catalase, superoxide dismutase, and glutathione peroxidase.[10–13] All these studies indicate that BXD may be a promising target as an anti-AD agent and has good application prospects in the clinical treatment of AD. Despite extensive research, AD remains an incurable disorder, with current therapies offering limited symptomatic relief. Traditional Chinese Medicine (TCM), such as BXD, may provide novel multi-target approaches.

The advent of the era of big data and artificial intelligence has seen systems pharmacology, including network pharmacology, molecular biology techniques, metabolomics, and transcriptomics, increasingly take a significant position in the field of medical research. These approaches combine experimental analysis with computational analysis.[14] TCM often contains multiple components that act on various targets and pathways. Network pharmacology, by constructing drug-target-disease networks, aids in elucidating the complex mechanisms of action of TCM formulas. Network pharmacology not only provides new perspectives and tools for TCM research but also contributes to the modernization and globalization of TCM.[15] Through this interdisciplinary collaboration, the potential of TCM in the prevention and treatment of diseases can be better explored and utilized. Metabolomics is a comprehensive systems approach for the analysis of small molecules in biological samples, and its application can provide clinically beneficial biomarkers.[16] The use of metabolomics is significant for disease diagnosis, investigation of disease mechanisms, and the selection of therapeutics. The combination of network pharmacology and metabolomics is expected to offer valuable technical support for studying the complex pathophysiology of AD.[17,18]

In this study, utilizing innovative ultra-high pressure liquid chromatography amalgamated with Q Exactive mass spectrometry (UHPLC-QE-MS), accompanied by high precision molecular docking methodologies, we deciphered the active components inherent in BXD. Subsequently, rigorous in vivo and in vitro assays substantiated BXD's neuroprotective efficacy against AD, delineating its mechanistic pathways and molecular interventions across both experimental realms. Finally, metabolomics analysis was performed in APP/PS1 mice after the treatment with BXD.

Materials and Methods

Network Pharmacology Analysis

Identification of active BXD ingredients and targets: Chemical components of BXD were collected using TCMSP (https://old.tcmsp-e.com/tcmsp.php), ETCM (http://bionet.ncpsb.org.cn/batman-tcm/index.php), HERB (http://herb.ac.cn/), SymMap (http://www.symmap.org/), and TCM-ID (https://www.bidd.group/TCMID/) databases respectively, selecting those with oral bioavailability ≥30% and drug-likeness ≥0.18. Disease-related targets were searched from

GeneCards (https://www.genecards.org/), OMIM (https://omim.org/), DrugBank (https://go.drugbank.com/), and CTD databases (http://ctdbase.org/), HPO (https://hpo.jax.org/app/), and the integration of disease-related targets was searched using "Alzheimer's disease" as the keyword. Using UniProt, we standardized and deduplicated drug target gene names to pinpoint potential disease targets. We employed Venn diagrams to illustrate target intersections across databases and identified common targets between our compound analysis and AD targets within R. These shared ingredients and targets, indicative of BXD's therapeutic impact on AD, are prioritized based on their Score value, with higher scores denoting greater disease relevance, for further analysis.

Construction and analysis of BXD-compound target-disease network: We imported the active ingredient-target correspondence of BXD into Cytoscape 3.9.1 to create a drug-compound-target-disease network. Nodes in this network represent compounds and targets, with edges indicating their interactions. Using the Network Analyzer plugin, we analyzed the network's topology, calculating node degrees to assess the connectivity and importance of each compound and target.

Construction and analysis of protein-protein interaction (PPI) network: We then constructed a PPI network using the STRING database (https://string-db.org/) to determine the interaction relationships among proteins related to BXD's therapeutic effects on AD. Core targets were identified using topological criteria such as closeness centrality (CC), betweenness centrality (BC), and degree ranking, which reflect the nodes' connectivity and influence in the network.

Network construction and Kyoto Encyclopedia of Genes and Genomes (KEGG) and Gene Ontology (GO): GO and KEGG pathway analyses were conducted using the bioinformatics platform (http://www.bioinformatics.com.cn) to investigate the enriched GO terms and KEGG pathways among the identified clusters. Enrichment was based on $P < 0.01$, which aided in predicting the biological processes and mechanisms involved in BXD's effects against AD. In GO enrichment analysis, $P < 0.05$ was selected as the screening condition, and the top 20 biological items whose $P < 0.05$ were selected to draw bar charts. KEGG enrichment analysis also took $P < 0.05$ as the significant enrichment screening condition, and the top 30 signal pathways with $P < 0.05$ were selected to draw bubble maps for visual analysis.

Constructing and Analyzing a Drug-Compound-Target-Pathway-Disease Network: To uncover the underlying mechanisms of drug action, we selected the core top-ranking pathways, along with their key targets and active ingredients, to construct a "drug-compound-target-pathway-disease" network. This network was designed to effectively illustrate the interconnections and synergistic effects between the drug's important active components and targets with certain significant pathways.

Molecular Docking: Selected compounds Stigmasterol, Acacetin, Nuciferin, Wogonin, Baicalein and Oroxylin a were subjected to molecular docking with the core targets Akt. The 3D structures of the primary active compounds were retrieved from the PubChem database, while the 3D structures of the core target proteins were obtained from the Protein Data Bank (PDB) (https://www.rcsb.org/). Preliminary processing of the core target proteins, including the removal of solvent molecules, was performed using PyMOL version 2.6.0. Subsequent hydrogenation and charge assignment were carried out using AutoDock Tools version 1.5.7. The core target proteins and active compounds were then saved as "pdbqt" formatted files, with appropriate grid positions and sizes set accordingly. The docking of the compounds and targets was ultimately completed using Autodock Vina. The docking results were visualized using PyMOL software.

Experimental Validation

Animals

The Jackson Laboratory supplied APPswe/PS1dE9 (APP/PS1) double transgenic mice (catalog number: 004462) for our study. These mice express a fusion of mouse and human amyloid precursor protein (Mo/HuAPP695swe) along with a variant of human presenilin 1.[19] The genotypic characterization of APP/PS1 double transgenic rodents was conducted following established protocols.[20] Adult Sprague-Dawley rats, each weighing approximately 200 ± 20 grams, were acquired from Jinan Pengyue Experimental Animal Breeding Co., LTD, Ethics Number:20230206–64. The Binzhou Medical University Hospital's Animal Ethics and Welfare Committee granted approval for all related animal studies, in strict adherence to the UK Animals (Scientific Procedures) Act of 1986. This compliance extends to the EU Directive for Animal Experiments [2010/63/EU] and the Guidelines for the Ethical Review of Laboratory Animal Welfare under the

People's Republic of China National Standard GB/T 35892–2018, ensuring that all procedures met or surpassed the required ethical standards for animal research.

BXD, BXD-Containing Serum Preparation, and Drug Administration

BXD formula granule were purchased from Kangrentang (Beijing, China), which is composed of seven Chinese herbs, the specific floristic sources and dosages are shown in Supplementary Table 1. They were dissolved in double-distilled H_2O at a concentration of 1.2 g/mL. For BXD-containing serum preparation, the rats were administered BXD (12 g/kg per day, oral gavage) for 7 consecutive days. Two hours subsequent to the administration on the seventh day, samples of blood were meticulously drawn from the abdominal aorta in a sterile fashion and subsequently subjected to a half-hour inactivation procedure at 56°C. The following step comprised filtration of these samples via a membrane with a 0.22 μm pore size. For conservation purposes and forthcoming analysis, we retained these samples at an extremely low-temperature setting of −80°C. This process operationalizes methods echoed in earlier approaches described in the scientific discourse.[21] APP/PS1 double transgenic mice (3 months old) were treated with BXD (12 g/kg per day, oral gavage) for 4 months. Our prior investigations have established the precise concentration for gavage administration.[9]

Identification of Active Components in BXD-Containing Serum Using UHPLC-QE-MS Analysis

UHPLC-QE-MS was used to detect the active ingredients of BXD-containing serum and was conducted by Beijing Baimike Biotechnology Co. LTD (Beijing, China). See Supplementary Materials and methods 1.

Cell Culture, $A\beta_{42}$ Preparation and Cell Viability Assay

The SH-SY5Y human neuroblastoma cell line, procured from the American Type Culture Corporation (Manassas, VA, USA), underwent cultivation in Dulbecco's Modified Eagle's Medium (DMEM) (Gibco, Waltham, MA, USA).This medium was enriched with a 10% concentration of fetal bovine serum and fortified with 1% penicillin-streptomycin, ensuring an optimal growth environment at a constant temperature of 37°C and a 5% CO_2 atmosphere. The amyloid-beta peptide $A\beta_{42}$, central to AD research, was initially solubilized in dimethyl sulfoxide. Subsequently, it was further diluted in DMEM to create a concentrated stock solution (10 μm), facilitating subsequent experimental investigations. Each well of a 96-well plate, occupied with SH-SY5Y cells, received an addition of CCK-8 (MedChemExpress, HY-K0301, China). The concentration of $A\beta_{42}$ is divided into 1μmol, 2μmol, 5μmol, 10μmol. This was followed by a subsequent 3-hour incubation period. Subsequently, absorbance at 450 nm was gauged utilizing a multifunctional microplate reader, guided by the manufacturer's manual. Vehicle + Vehicle: Represents normal cells subjected to serum deprivation in DMEM for 48 hours, followed by treatment with normal rat serum for an additional 48 hours. Aβ + Vehicle: Represents normal cells treated with 5 μM Aβ42 in DMEM for 48 hours, followed by treatment with normal rat serum for an additional 48 hours. Aβ+BXD (10%): Represents normal cells treated with 5 μM Aβ42 in DMEM for 48 hours, followed by treatment with 10% BXD-containing serum for 48 hours. Aβ+BXD (15%): Represents normal cells treated with 5 μM Aβ42 in DMEM for 48 hours, followed by treatment with 15% BXD-containing serum for 48 hours. This grouping design maximizes the unity of molding factors and drug administration factors and reduces the influence of other factors.

Immunofluorescence

The SH-SY5Y cells were fixed with 4% paraformaldehyde before being permeabilized with Triton X-100 (0.5%) for half an hour. Subsequently, they were blocked using 5% donkey serum and then incubated with primary antibody against NeuN (1:500) overnight at 4 °C. After extensive washing with phosphate-buffered saline (PBS), the cells were incubated with Alexa Fluor®488 goat anti-rabbit IgG secondary antibodies (1:400, A21202, Invitrogen) for 4 h and visualized using an Olympus FV1000 confocal microscope (Olympus, Shinjuku, Tokyo, Japan). The number of NeuN-positive cells from six randomly selected fields per group was calculated by researchers who were blinded to the experimental design.

Ethynyl-2′-Deoxyuridine (EDU) Staining

In this experiment, 100 μL of 50 μM Edu solution (C0071S, Beyotime, Shanghai, China) was added to each well of 24-well plates for 2 h. Subsequently, the concentrated cells were fixed in situ, employing a 4% solution of paraformaldehyde, over a quarter-hour duration.Following this fixing phase, a 10-minute permeabilization process ensued, using 0.5% TritonX-100 as the permeabilizing agent. The final step involved incubating the cells with 100 μL of Apollo reaction mix, executed under exclusion of light for half an hour. Subsequently, the cells underwent a permeabilization process for a duration of 10 minutes, employing 0.5% TritonX-100. This was followed by an incubation period where 100 μL of Apollo reaction solution was introduced, conducted under dark conditions lasting half an hour. Cell nuclei were stained with Hoechst 33342. Images were captured using an Olympus FV1000 confocal microscope (Olympus), and the number of positive cells from six randomly selected fields per group was calculated by researchers who were blinded to the experimental design.

Scratch Healing Assay

The cells were inoculated into 6-well plates. After 24 h, the cells were scraped using a 200-μL tip, incubated with 2% drug-containing serum, and cultured at 37 °C and 5% CO_2 for 24 h or 48 h. Photomicrographs were taken before and after treatment using an optical microscope (IX53; Olympus). The relative distance of the wound width before treatment minus the wound width after treatment was calculated and quantified using ImageJ software (http://imagej.nih.gov/ij/).

Reverse Transcription Quantitative Polymerase Chain Reaction (RT-qPCR)

Adopting established protocols, cellular total RNA was isolated utilizing TRIzol reagent (Invitrogen, Carlsbad, CA, USA),[22] subsequently undergoing reverse transcription into cDNAs with the assistance of a cDNA synthesis kit (Thermo Scientific, Waltham, MA, USA). The cDNA underwent examination via the StepOnePlus real-time PCR mechanism (Applied Biosystems, Waltham, MA, USA). GAPDH served as the standardizing reference. The PCR primer pairs used were: BCL-2: forward: 5′-GCTACCGTCGTGACTTCGC-3′, reverse: 5′-CCCCACCGAACTCAAAGAAGG-3′; caspase 3: forward: 5′-TGAAGGGGTCATTTATGGGACA-3′, reverse, 5′-CCAGTCAGACTCCGGCAGTA-3′; IL-1β: forward, 5′-GAAATGCCACCTTTTGACAGTG-3′, reverse, 5′-TGGATGCTCTCATCAGGACAG-3′; TNF-α: forward, CTGAACTTCGGGGTGATCGG-3′, reverse, 5′-TGGATGCTCTCATCAGGACAG-3′; IL-6: forward, 5′-TCTATACCACTTCACAAGTCGGA-3′, reverse, 5′-GAATTGCGGCTTGTCACTCGAATTTTGAGA-3′. Relative target gene quantification was performed using the $2^{-\Delta\Delta CT}$ method.

Western Blot Analysis

Total protein was extracted from samples after different treatments as previously described.[23] Total proteins were separated using SDS-PAGE and transferred to PVDF membranes (Millipore, Billerica, Massachusetts, USA). The membrane was subjected to a blocking process involving 5% skim milk powder dissolved in TBST buffer, composed of 20 mm Tris-HCl at pH 7.4, 150 mm NaCl, and 0.1% Tween 20. Subsequently, it was exposed to specific primary antibodies, which were diluted in the same blocking medium, for an extended period at 4 °C, typically overnight: p-Akt (66444-1-Ig, Proteintech, 1:1000), Akt (60203-2-Ig, Proteintech, 1:1000), IL-6 (CQA3710, Abways, 1:1000), pro-IL-1β/IL-1β (12242, CST, 1:1000), TNF-α (AB3558, Abways, 1:1000), Bcl-2 (27888S, CST, 1:1000), caspase 3 (3033T, CST, 1:1000), Cleaved-caspase (9664T, CST, 1:1000), Bax (EPR18283, Abcam, 1:1000), ASC (A15093, Nature Biosciences, 1:1000), NLRP3 (A10997, Nature Biosciences, 1:1000) and β-actin (AY0573, Abways, 1:10,000). This was followed by incubation with goat anti-rabbit IR Dye 680LT (1:5000, #926-68021; Li-COR Biosci-ences, Lincoln, NE, USA) or goat anti-mouse IR Dye 800CW (1:5000, #926-32210; Li-COR Biosciences) fluorescent secondary antibodies. Fluorescence was captured and quantified using an Odyssey infrared imaging system (Li-COR Biosciences, Lincoln, NE, USA).

Enzyme-Linked Immunosorbent Assay (ELISA)

SY5Y cells were seeded in 6-well plates. Upon completion of the various treatments, cellular supernatant was subjected to centrifugation at a rate of 1000 rpm/min for a half hour. Subsequently, the liquid residue was extracted with the aim of examining the release of TNF-α, IL-6, and IL-1β. This was accomplished utilizing Enzyme-Linked Immunosorbent

Assay kits (EK0525-96, EK0410-96T, EK0392, Boster, Wuhan, China) and complying meticulously with the guidelines provided by the manufacturer.

Flow Cytometry Analysis

After multiple interventions, SY5Y cells were collected and suspended in PBS. Subsequently, they were subjected to staining with Annexin V-FITC and propidium iodide (PI) in sequence. This was followed by an analysis utilizing the FITC Annexin V apoptosis detection kit, adhering strictly to the guidelines provided by the manufacturer (556547; BD Biosciences, Franklin Lakes, NJ, USA).

Y-Maze

The three arms of the Y-maze were separated at 120° angles and randomly set as A, B, and C, each marked with a black strip or dotted paper. The rodents were situated at the terminus of a designated corridor, permitted to conduct an uninhibited investigation spanning a duration of precisely 600 seconds. The total number of entries into each arm and the total number of alternations (defined as the total number of triple strings containing three consecutive arm serial numbers) were counted. The percentage of spontaneous alternations (SAP) can be calculated through the equation: SAP (%) = [Quantity of Alternations / (Sum of Arm Entries - 2)] × 100.[20]

Novel Object Recognition (NOR)

The NOR test was divided into two phases. Initially, throughout the preparatory stage, the rodent subjects were positioned within the research apparatus containing two homogenous artifacts and granted an exploration duration of a ten-minute interval. Following a 2-hour sequestration phase (denoted as NOR-2h), the rodents were reintroduced to their environment, prompting the replacement of the pre-existing items with new and intriguing elements. Subsequently, the experimental procedure was replicated following an intermission of 24 hours (denoted as NOR-24 h). The quantification of the time allocated to each subject was derived from the proportion of time concurrently dedicated to scrutinizing two entities.

H&E Staining

For histopathological analysis, tissue embedded in paraffin was sectioned at 4 μm thickness, dewaxed in xylene, and rehydrated through a graded ethanol series. Following rinsing, sections were stained with Hematoxylin and Eosin, dehydrated in absolute ethanol, and cleared in xylene. The slices were observed under a × 20 objective lens of an optical microscope.

Metabolomics Analyses

The metabolomics experiments were performed by Genechem Co., Ltd (Shanghai, China). Supplementary Materials and methods 2.

Statistical Analysis

The results are expressed as means ± standard errors of the means (SEMs). The data were analyzed with GraphPad Prism version 9.0.0. The assumptions of normality and uniform variance were examined through the implementation of the Shapiro–Wilk and F statistical trials. To compare normally distributed data between groups, two-tailed unpaired t-tests were used. We executed an array of collective examinations via single-direction variance analyses (ANOVAs), succeeded by post-hoc assessments using Sidak's method. For data disallowed from a normal distribution, we applied the Kruskal–Wallis test, followed by Dunn's process for comparative analysis. The statistical significance was affirmed at $p < 0.05$.

Results

Utilizing Network Pharmacology and UHPLC-QE-MS Analysis Identified the Key Components of BXD Anti-AD

Our analysis of multiple databases revealed that 256 action targets were retrieved from the ingredients of BXD, meanwhile, 952 targets were associated with AD were found. The intersection of BXD with AD-related 139 potential targets (Figure 1A), accompanied by concrete information on the top 20 active components of BXD (Supplementary Table 2).

Next, UHPLC-QE-MS was used to identify the chemical components of BXD and BXD drug-containing serum. A total of 56 chemical components were found in the BXD drug-containing serum (Supplementary Table 3) after excluding background interference from the blank serum. The total ion chromatogram of BXD is shown in Figure 2A and 2B, and a heat map of the main ingredients is shown in Figure 2C. Furthermore, the combined overlapped screening of BXD targets derived from network pharmacology and UHPLC-QE-MS strategy analysis of BXD drug-containing serum resulted in the acquisition of six main components, including wogonin, baicalein, nuciferin, acacetin, oroxylin A, and stigmasterol, which were labeled in our mass spectra (Figure 2A-B, Supplementary Table 4).

Neuroprotective Effect of BXD on $A\beta_{42}$-Induced Cytotoxicity in vitro

We evaluated the efficacy of BXD on $A\beta_{42}$-induced neurotoxicity in SY5Y cells. First, we screened the optimal modeling concentration of $A\beta_{42}$ intervention in SY5Y cells. We observed that incubation with 5 μm $A\beta_{42}$ produced obvious and stable cytotoxicity at 48 h, which was selected for subsequent experiments (Figure 3A). Furthermore, immunofluorescence results revealed that Aβ42 treatment dramatically decreased the numbers of NeuN-positive cells ($p < 0.01$), while both 10% and 15% BXD drug-containing serum increased the number of NeuN-positive cells, exhibiting reparative effects on $A\beta_{42}$-induced cytotoxicity in SY5Y cells ($p < 0.05$, $p < 0.01$). The cell viability results indicated a decreased viability after $A\beta_{42}$ treatment, which was reversed by the application of 10% and 15% BXD-containing serum ($p < 0.05$, $p < 0.01$). Cell migration is an important process in many physiological and pathological processes.[24] $A\beta_{42}$ intervention suppressed the chemotactic and migratory activity of SY5Y cells (Figure 3E, $p < 0.05$, $p < 0.01$). Different doses of BXD-containing serum showed no improved effect on this decline at 24 h after incubation, while 15% BXD drug-containing serum prevented this decline at 48 h after incubation ($p < 0.05$, $p < 0.01$). In addition, Edu staining confirmed that the BXD drug-containing serum significantly reversed the restrained proliferation of SY5Y cells induced by $A\beta_{42}$ exposure (Figure 3F, $p < 0.05$).

BXD Regulated Neuroinflammation and Apoptosis in $A\beta_{42}$-Induced SY5Y Cells

In order to decipher the intricate processes through which BXD influences AD, we utilized the STRING database as a scientific tool to dissect the protein-protein interaction (PPI) network associated with potential BXD targets against AD. The top 30 targets were extracted based on the degree value ranking (Figure 4A-B, Supplementary Table 5), including tumor protein 53 (TP53), protein kinase B 1 (AKT1), JUN, heat shock protein 90 alpha family class A member 1 (HSP90AA1), estrogen receptor alpha gene (ESR1), b-cell lymphoma 2 (BCL-2), REL-associated protein (RELA), interleukin 6 (IL-6), caspase 3 (CASP3). Among them, inflammatory factors and apoptosis indicators constitute the majority.Neuroinflammation and apoptosis were reported to be key pathological aspects involved in the $A\beta_{42}$-induced cytotoxicity.[25] NLRP3 inflammasome is intricately linked to neuroinflammation through its activation by DAMPs, subsequent caspase-1 activation, and the release of pro-inflammatory cytokines. It contributes to neuronal damage and death, making it a critical component in the pathogenesis of AD.[26] Therefore, we evaluated some pro-inflammatory factors and apoptosis-related markers to verify the potential changes in neuroinflammation and apoptosis in $A\beta_{42}$-induced SY5Y cells. The findings of the WB analysis illustrated a substantial elevation in the protein concentrations of TNF-α, IL-6, IL-1β, and NLRP3 inflammasome (ASC, Caspase-1, and pro-IL-1β) in the $A\beta_{42}$ group, when juxtaposed with the control group, while 10% and 15% BXD drug-containing serum attenuated this elevation (Figure 4C-I, $p < 0.05$, $p < 0.01$). ELISA results demonstrated a significant inhibitory effect of 10% and 15% BXD drug-containing serum on the abnormal elevation of TNF-α, IL-6, and IL-1β levels after $A\beta_{42}$ treatment ((Figure 4J-L, $p < 0.05$, $p < 0.01$).

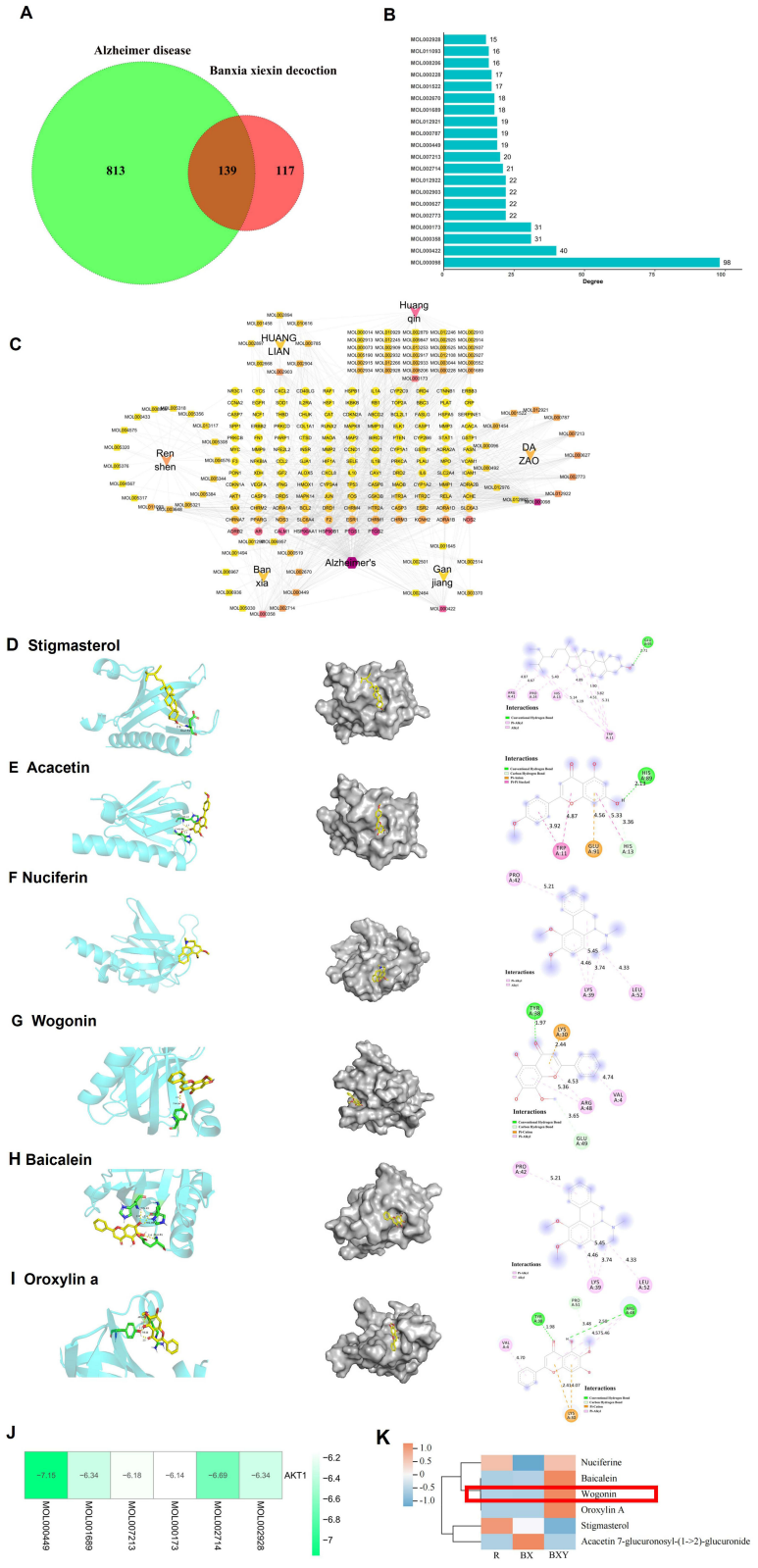

Figure 1 Network analysis of BXD in the treatment of AD. (**A**) Venn diagram of predicted targets of BXD and AD. (**B**) The ranking of BXD target components importance for treating AD. (**C**) BXD-components-active ingredients-potential targets-pathways network. Molecular models of the binding of Stigmasterol (**D**), Acacetin (**E**), Nuciferin (**F**), Wogonin (**G**), Baicalein (**H**), and Oroxylin A (**I**). (**J**) Heat map of molecular docking results. (**K**) Heat map of the distribution of main components in BXD-containing serum. (**R**) Normal rat serum, BX: BXD-containing serum, BXY: BXD drugs.

https://doi.org/10.2147/DDDT.S499852

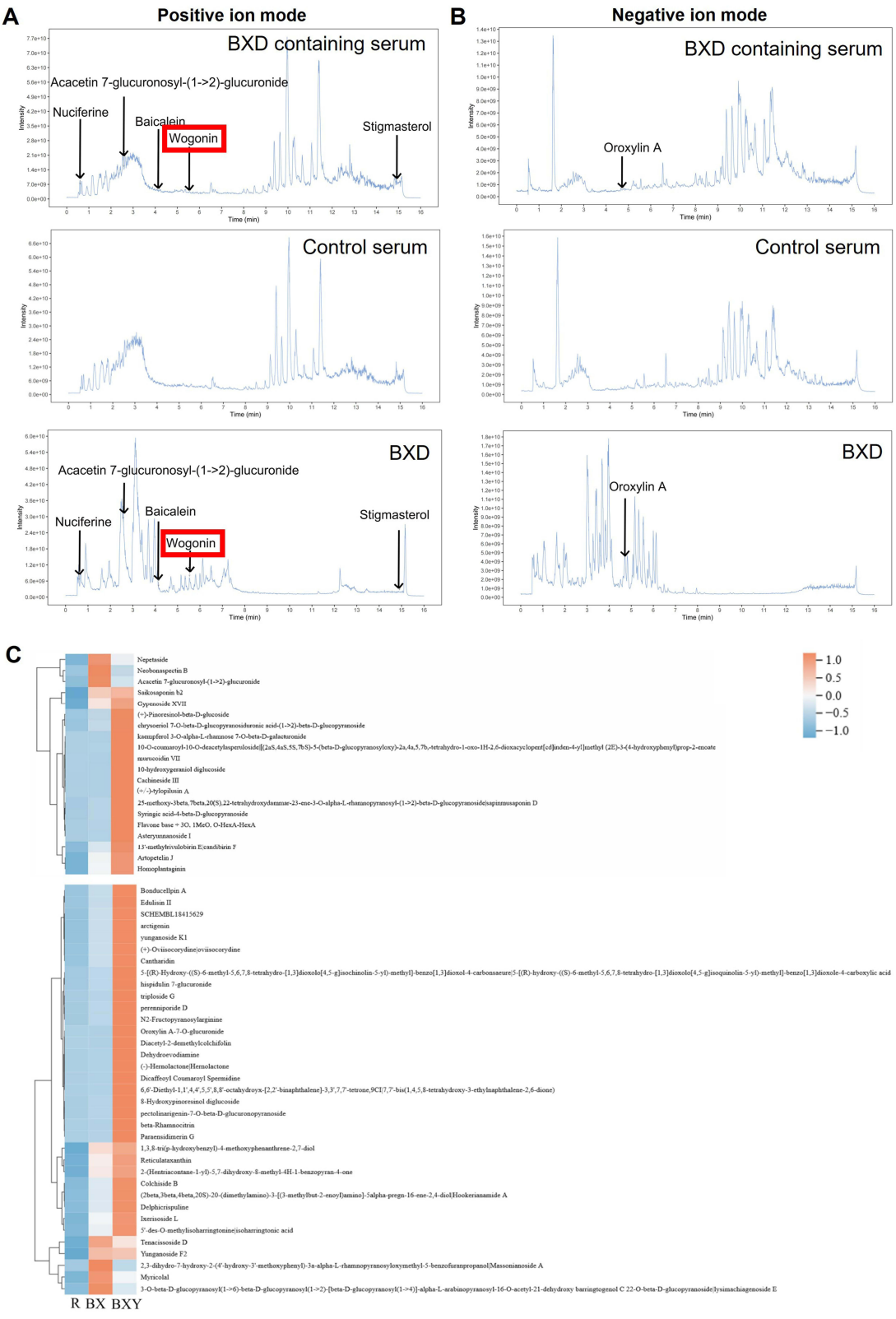

Figure 2 Total ion chromatograms of BXD-containing serum. (**A**) Total ion flow pattern in positive ion mode. (**B**) Total ion flow pattern in negative ion mode. (**C**) Heat map of the components of BXD-containing serum.

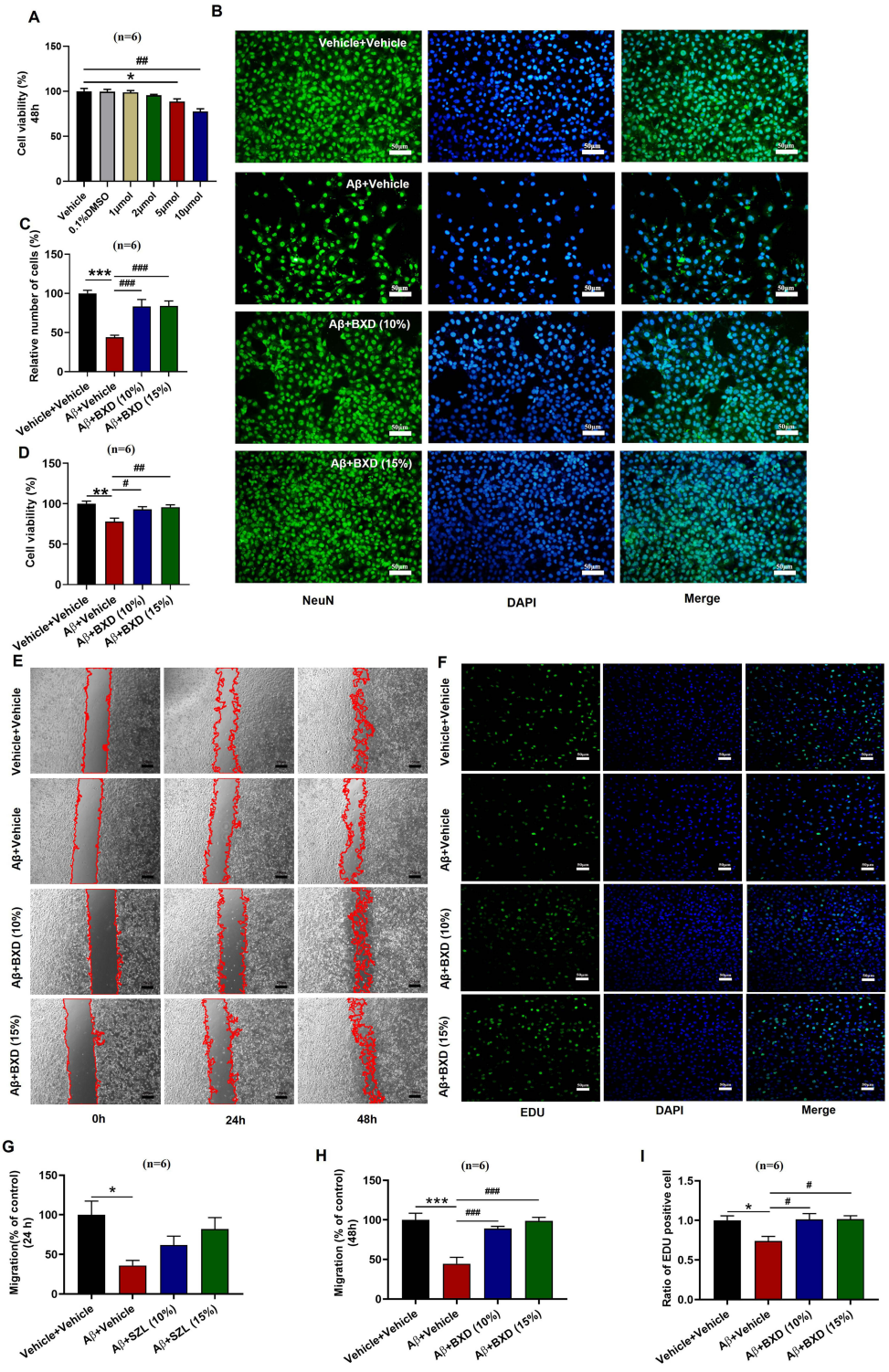

Figure 3 Effect of BXD-containing serum on viability of SY5Y cells stimulated by $A\beta_{42}$. (**A**) CCK-8-mediated detection of optimum molding dosage of $A\beta_{42}$ on SH-SY5Y cell for 48 h. (**B** and **C**) Representative images and statistical analysis of fluorescence analysis of NeuN (scale bar = 50 μm). (**D**) Effect of BXD-containing serum on $A\beta_{42}$-stimulated cell viability in SH-SY5Y cells. (**E, G**) Representative images and statistical analysis of SY5Y cell migration via in vitro wound healing assay (scale bar= 50 μm). (**F, H** and **I**) Representative images and statistical analysis of Edu staining (scale bar = 50 μm). All data are presented as means ± SEM (n=6). **p*<0.05, ***p*<0.01, versus Control group, #*p*<0.05, ##*p*<0.01 versus Model group; Used one-way ANOVA for *p*-value calculation. Vehicle + Vehicle: Represents normal cells subjected to serum deprivation in DMEM for 48 hours, followed by treatment with normal rat serum for an additional 48 hours. Aβ + Vehicle: Represents normal cells treated with 5 μM Aβ42 in DMEM for 48 hours, followed by treatment with normal rat serum for an additional 48 hours. Aβ+BXD (10%): Represents normal cells treated with 5 μM Aβ42 in DMEM for 48 hours, followed by treatment with 10% BXD-containing serum for 48 hours. Aβ+BXD (15%): Represents normal cells treated with 5 μM Aβ42 in DMEM for 48 hours, followed by treatment with 15% BXD-containing serum for 48 hours.

https://doi.org/10.2147/DDDT.S499852

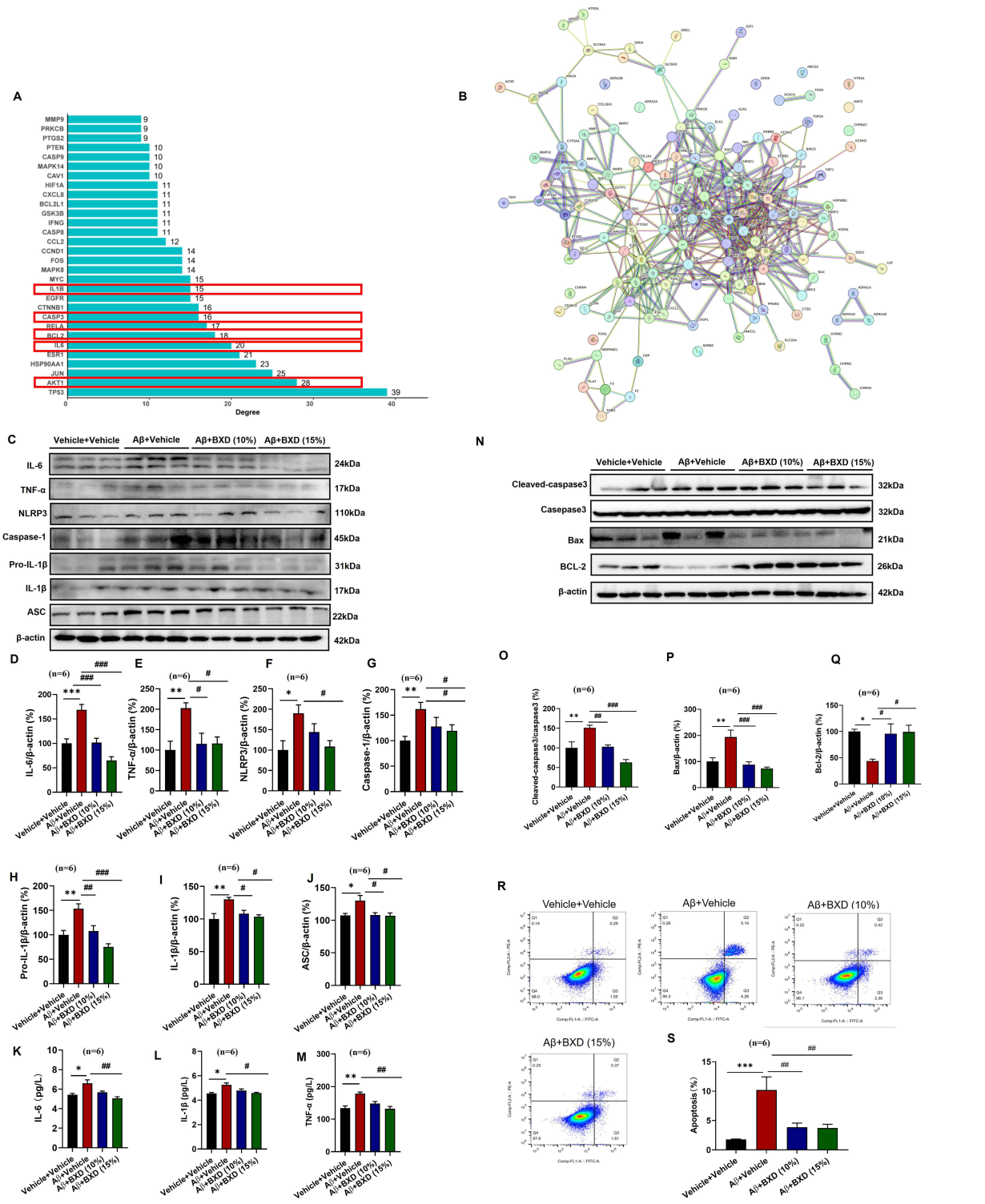

Figure 4 Effect of BXD-containing serum on pro-inflammatory factors and apoptosis. (**A**) The ranking of BXD target genes importance for treating AD. (**B**)The PPI networks of BXD. (**C–I**) Representative blots and quantitative data of IL-6, TNF-α, NLRP3, pro-IL-1β, IL-1β, and ASC. (**J–L**) ELISA for IL-6, IL-1β, and TNF-α. (**M–P**) Representative blots and quantitative data of cleaved-caspase 3, BCL-2, and BAX. (**Q**) Flow cytometry scatter plot. Q1: mechanically damaged cells, Q2: inactive cells, Q3: early apoptotic cells, Q4: live cells; cell apoptosis rate (%) = Q2 + Q3. (**R**) Quantitative data of flow cytometry. All data are presented as means ± SEM (n=6). *p<0.05, **p<0.01, versus Control group, #p<0.05, ##p<0.01 versus Model group; Used one-way ANOVA for p-value calculation. Vehicle + Vehicle: Represents normal cells subjected to serum deprivation in DMEM for 48 hours, followed by treatment with normal rat serum for an additional 48 hours. Aβ + Vehicle: Represents normal cells treated with 5 μM Aβ42 in DMEM for 48 hours, followed by treatment with normal rat serum for an additional 48 hours. Aβ+BXD (10%): Represents normal cells treated with 5 μM Aβ42 in DMEM for 48 hours, followed by treatment with 10% BXD-containing serum for 48 hours. Aβ+BXD (15%): Represents normal cells treated with 5 μM Aβ42 in DMEM for 48 hours, followed by treatment with 15% BXD-containing serum for 48 hours.

This exposition seeks to elucidate whether the compound BXD mitigates $A\beta_{42}$-induced cell death in SY5Y cells. This is ascertained through the investigation of key apoptotic markers, including cleaved-caspase 3, Bcl-2, and Bax protein expression levels. $A\beta_{42}$ increased protein expression levels of cleaved-caspase 3 and Bax and decreased protein expression levels of Bcl-2 ($p < 0.05$, $p < 0.01$). However, BXD-containing serum significantly improved this effect (Figure 4M-P, $p < 0.05$, $p < 0.01$). Moreover, flow cytometry analysis was performed to identify the significant anti-apoptotic effect of different doses of BXD-containing serum induced by $A\beta_{42}$ treatment (Figure 4Q-R, $p < 0.05$, $p < 0.01$).

BDX Modulated PI3K/Akt Signaling Pathways via Molecular Docking Mediated Analysis and Experimental Verification

GO and KEGG analyses were performed on the 139 intersection targets to evaluate their common biological functions and pathways. GO functional enrichment analysis showed 140 cell component (CC), 2631 biological process (BP), and 239 molecular function (MF) enrichment items. KEGG pathway enrichment analysis identified 182 significant signaling pathways. The top 20 related functions with high CC, BP and MF were ranked from high to low according to the number of enriched targets. These functions included response to xenobiotic stimulus, cellular response to chemical stress, response to oxidative stress, response to reactive oxygen species, response to metal ion, response to lipopolysaccharide, cellular response to oxidative stress, response to molecule of bacterial, response to radiation, response to peptide, response to oxygen levels, wound healing, response to decreased oxygen levels, regulation of apoptotic signaling pathway, response to hypoxia, response to UV, neuron death, gland development, reactive oxygen species metabolic process, response to light stimulus, membrane raft, membrane microdomain, caveola, plasma membrane raft, postsynaptic membrane, integral component of postsynaptic membrane, intrinsic component of postsynaptic membrane, secretory granule lumen, serine protease inhibitor complex, integral component of synaptic membrane, G protein-coupled amine receptor activity, catecholamine binding, D-binding transcription factor binding, R polymerase ll-specific D-binding transcription, adrenergic receptor activity, heme binding, neurotransmitter receptor activity, tetrapyrrole binding, alpha-adrenergic receptor activity, dopamine binding, postsynaptic neurotransmitter receptor activity, ubiquitin-like protein ligase binding, G protein-coupled serotonin receptor activity, serotonin receptor activity, ubiquitin protein ligase binding, transcription coregulator binding, dopamine neurotransmitter receptor activity, estrogen 2-hydroxylase activity, protein phosphatase binding, cytokine receptor binding. It encompasses a multitude of functions related to neurons and synapses.

KEGG pathway enrichment analysis revealed the potential targets of BXD against AD, and the Top 30 pathways in terms of significance were selected for analysis, which were concentrated in the PI3K/Akt, AGE-RAGE, IL-17 and TNF signaling pathways (Figure 5A, Supplementary Table 6). In terms of enrichment extent, the PI3K/Akt pathway shows a high level of enrichment, leading us to infer that the PI3K/Akt signaling pathway plays a significant role in the therapeutic effects of BXD on AD. The Akt-mediated pathway has received special attention among the top pathways derived from KEGG pathway enrichment analysis. The serine/threonine protein kinase, commonly referred to as Akt, plays a pivotal role in an array of biological mechanisms including, but not limited to cellular propagation, inflammation, and assorted forms of metabolism[27] Recent studies have shown that Akt is involved in various mechanisms of AD pathogenesis.[28] The molecular docking results showed that AKT has a strong binding ability with the 6 main components of BXD: stigmasterol (−7.15 kcal/mol), acacetin (−6.34 kcal/mol), nuciferin (−6.18 kcal/mol), wogonin (−6.14 kcal/mol), baicalein (−6.69 kcal/mol), and oroxylin A (−6.34 kcal/mol).

Furthermore, our validation results revealed that $A\beta_{42}$ led to lower protein expression levels of p-PI3K, p-Akt ($p <0.05$) and higher protein expression levels of p-NF-κB, while BXD-containing serum rescued this phenotype ($p < 0.05$, $p < 0.01$). Finally, an interactive map of the PI3K/Akt pathway was generated to determine whether there are multiple signaling pathways or molecular targets underlying the regulatory function of Akt (Figure 5D-G).

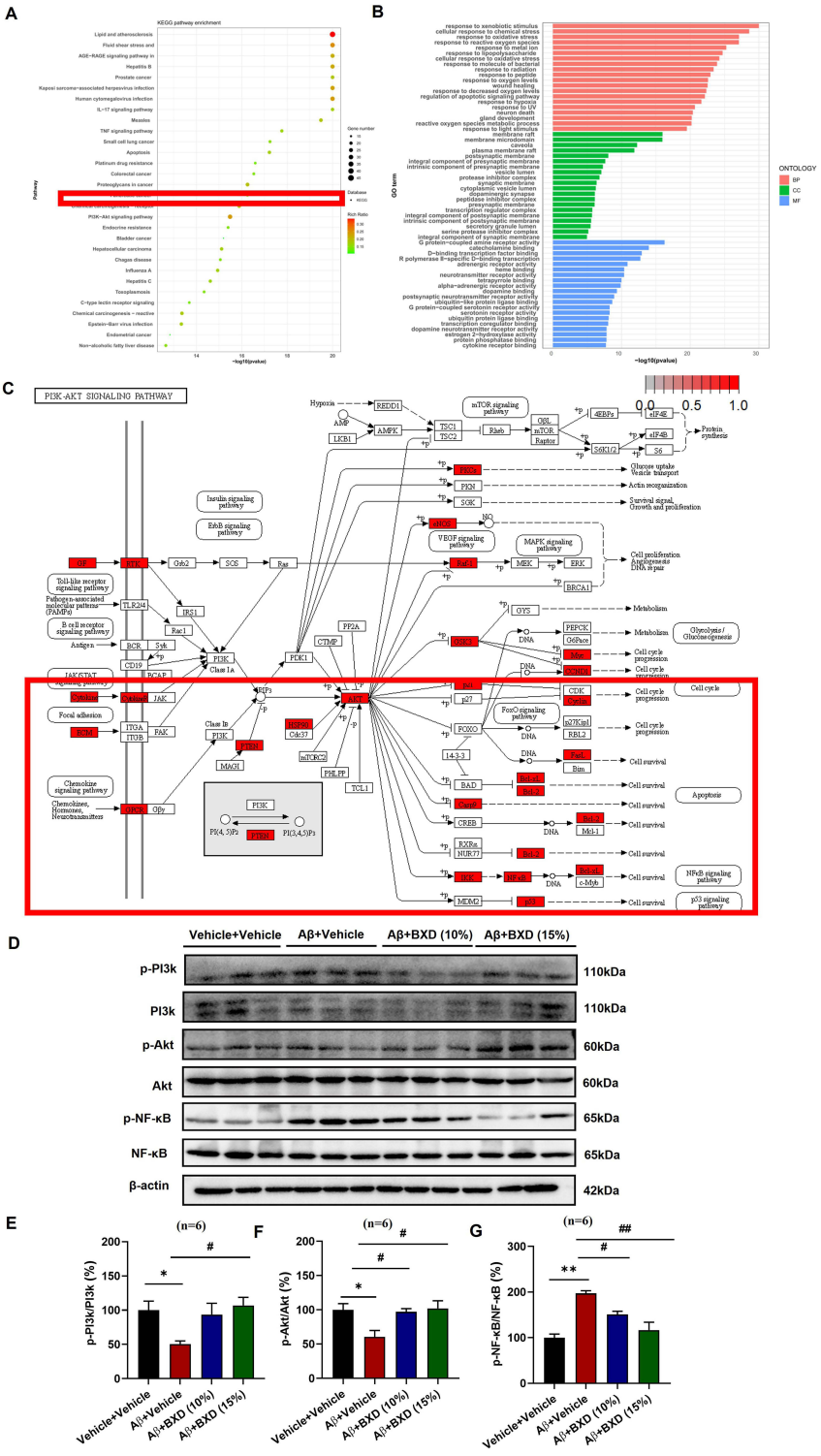

Figure 5 Effect of BXD-containing serum on the PI3K/Akt signaling pathway. (**A**) The identified top 30 KEGG pathways. (**B**) The analyzed top 60 GO terms. CC: Cellular component category. BP: Biological process category. MF: Molecular function category. (**C**) Interactive map analysis of the PI3K/Akt pathway. (**D** and **E**) Representative blots and quantitative data of p-PI3K, p-Akt, p-NF-κB. All data are presented as means ± SEM (n=6). *p<0.05, **p<0.01, versus Control group, #p<0.05, ##p<0.01 versus Model group; Used one-way ANOVA for p-value calculation. Vehicle + Vehicle: Represents normal cells subjected to serum deprivation in DMEM for 48 hours, followed by treatment with normal rat serum for an additional 48 hours. Aβ + Vehicle: Represents normal cells treated with 5 μM Aβ42 in DMEM for 48 hours, followed by treatment with normal rat serum for an additional 48 hours. Aβ+BXD (10%): Represents normal cells treated with 5 μM Aβ42 in DMEM for 48 hours, followed by treatment with 10% BXD-containing serum for 48 hours. Aβ+BXD (15%): Represents normal cells treated with 5 μM Aβ42 in DMEM for 48 hours, followed by treatment with 15% BXD-containing serum for 48 hours. This grouping design maximizes the unity of molding factors and drug administration factors and reduces the influence of other factors.

 https://doi.org/10.2147/DDDT.S499852

BXD Improved the Cognitive Function, Neuroinflammation, and Apoptosis in vivo

To verify the therapeutic ability of BXD against AD-related cognitive damage, we selected 3-month-old APP/PS1 mice, as this is the age of onset of learning memory deficits.[20] These mice were administered BXD via intragastric infusion for 4 months, and Y-maze and NOR experiments were performed to evaluate learning memory behaviors (Figure 6A). We used HE staining to measure neurons in the hippocampus of mice. The number of neurons in the APP/PS1 mice decreased a compared with control group. The injured neurons in BXD group were repaired to some extent, the cells were closely arranged compared with model group (Figure 6B). In the Y-maze test, BXD treatment reliably improved spatial working memory, as demonstrated by increased spontaneous alternations (Figure 6C, $p < 0.05$). In the NOR test, BXD treatment significantly increased the time spent on novel object investigation in both the 1 h ($p < 0.01$) paradigms. BXD mitigates AD-associated neuroinflammation by downregulating key pro-inflammatory cytokines (IL-6, IL-1β, TNF-α), as observed in APP/PS1 mice. Moreover, BXD improved the expression of apoptosis-related indicators (Caspase 3, Bcl-2, Bax). These results demonstrated that BXD plays an anti-amnesic role in AD mice by regulating inflammation and apoptosis.

Integrated Analysis of Metabolomics of BXD-Induced APP/PS1 Mice

In our quest to unearth the underlying mechanisms accountable for BXD's influence on cognitive debility, we conducted untargeted metabolomics analysis in both negative and positive ion modes. By this approach, we gauged alterations in plasma metabolomics in APP/PS1 mice treated with BXD. PCA relies on orthogonal transformation to achieve dimensionality reduction using an unsupervised data analysis method.[29] PCA and PCA 3D map results showed that the metabolic components in the plasma of BXD-treated APP/PS1 mice were significantly different from those in unmodified mice (Figure 7A and B). In our study, we discerned 502 and 364 distinct metabolites within serum samples using positive and negative modes, respectively. Employing Partial Least Squares Discriminant Analysis (PLSDA), we effectively isolated and delineated metabolic variations, leveraging the holistic traits of the raw dataset. The parameters defining the model's quality indicated a coefficient of determination (R2) amounting to 1.00 and a predictive residual sum of squares (Q2) attaining 0.77 during positive ionization. Simultaneously, the metrics for negative ionization yielded an R2 value of 1.00 and a Q2 score of 0.80. As depicted in Figure 7E, the cluster analysis heatmap of AD associated metabolites reveals a notable enhancement in the expression of elements such as wogonin, berberine, diflorasone and glycitein brought about by BXD. Utilizing network pharmacology, metabolomics, and UHPLC-QE-MS analysis, we have identified Wogonin as a key component of BXD that contributes to its anti-AD effects (Figures 1K and 2A). Simultaneously, a substantial suppression in the expression levels of L-cysteine, aminoimidazole carboxamide ribonucleotide, phenylacetylglycine among others is observed (Figure 7C). The affected pathways in the plasma were mainly involved in phenylalanine metabolism, tyrosine in positive and negative ionization (Figure 7D).

Discussion

Network pharmacology offers several advantages in the study of TCM, which is characterized by a multi-component, multi-target, and integrative efficacy approach.[30] It integrates clustering algorithms with network topology to construct intricate relationships among components, targets, and diseases, predicated on compound-target protein interactions.[31] Consequently, by employing network pharmacology, we have pinpointed the most promising gene targets for BXD treatment in AD, with key targets emerging that offer a more nuanced comprehension of the mechanisms underlying this study.

Moreover, an examination of the KEGG pathways highlighted that the PI3K/Akt, TNF, AGE-RAGE, and IL-17 signaling routes emerged as significantly responsive pathways potentially modulated by BXD in the treatment of AD. The PI3K/Akt pathway is a critical regulator of cell survival, metabolism, and synaptic plasticity.[32] In AD, this pathway is often dysregulated, leading to increased neuronal apoptosis and impaired synaptic function. Activation of the PI3K/Akt pathway can promote cell survival by inhibiting pro-apoptotic proteins and enhancing glucose metabolism, which is crucial for maintaining neuronal health.[33] The AGE-RAGE pathway is implicated in the development of neuroinflammation and oxidative stress, both of which are key pathological features of AD. AGEs can bind to RAGE receptors on

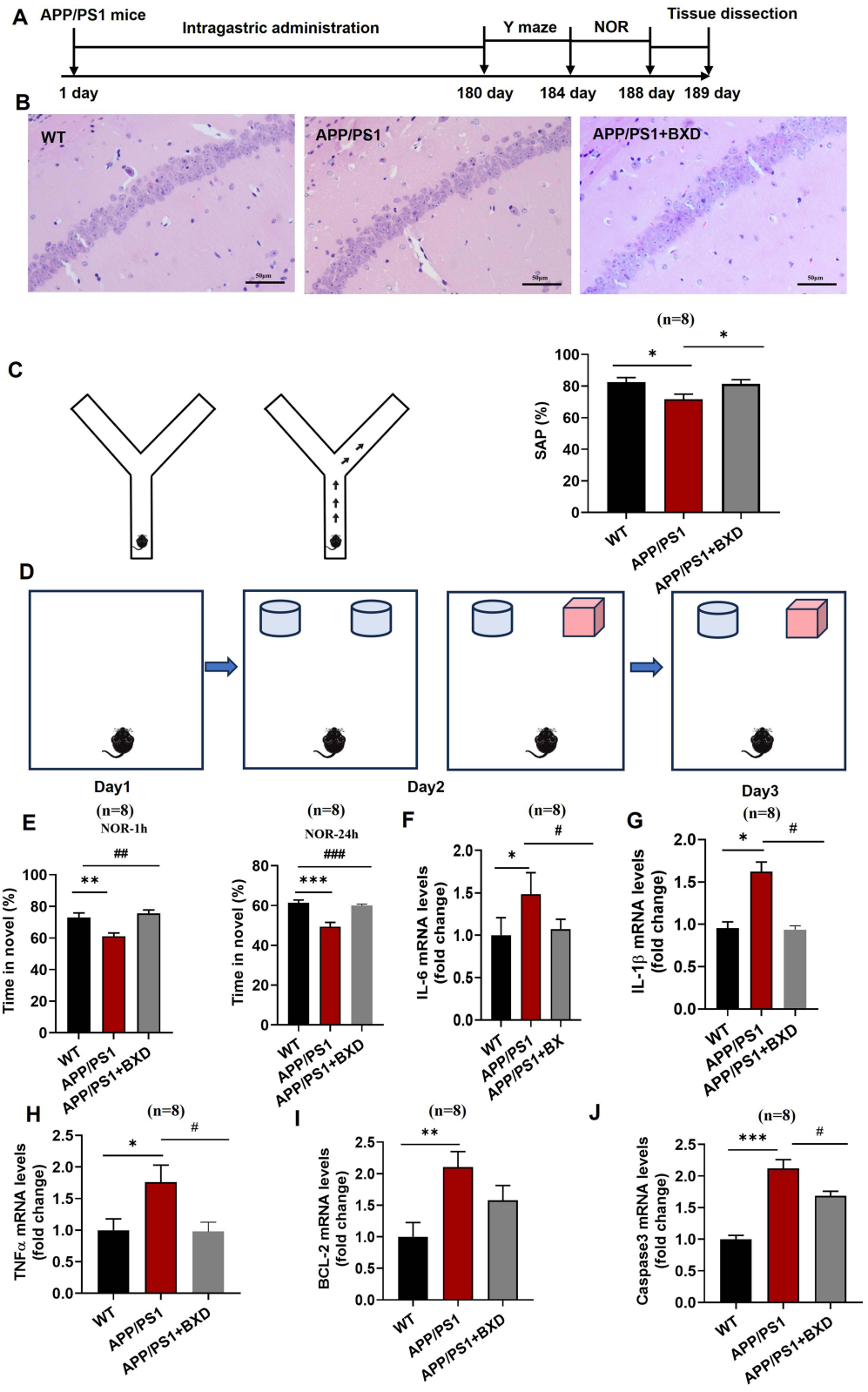

Figure 6 Role of BXD in alleviating cognitive deficits and memory disabilities in APP/PS1 mice. (**A**) Experimental design. (**B**) Y-maze model diagram. (**C**) Measurement of SAP %. (**D**) NOR model diagram. (**E**) Measurement of NOR-1 h, NOR-24 h. Statistical analysis of mRNA expression of IL-6 (**F**), IL-1β (**G**), TNF-α (**H**), BCL-2 (**I**), and caspase 3 (**J**). All data are presented as means ± SEM (n=8). **p*<0.05, ***p*<0.01, versus Control group, #*p*<0.05, ##*p*<0.01 versus Model group; Used one-way ANOVA for *p*-value calculation.

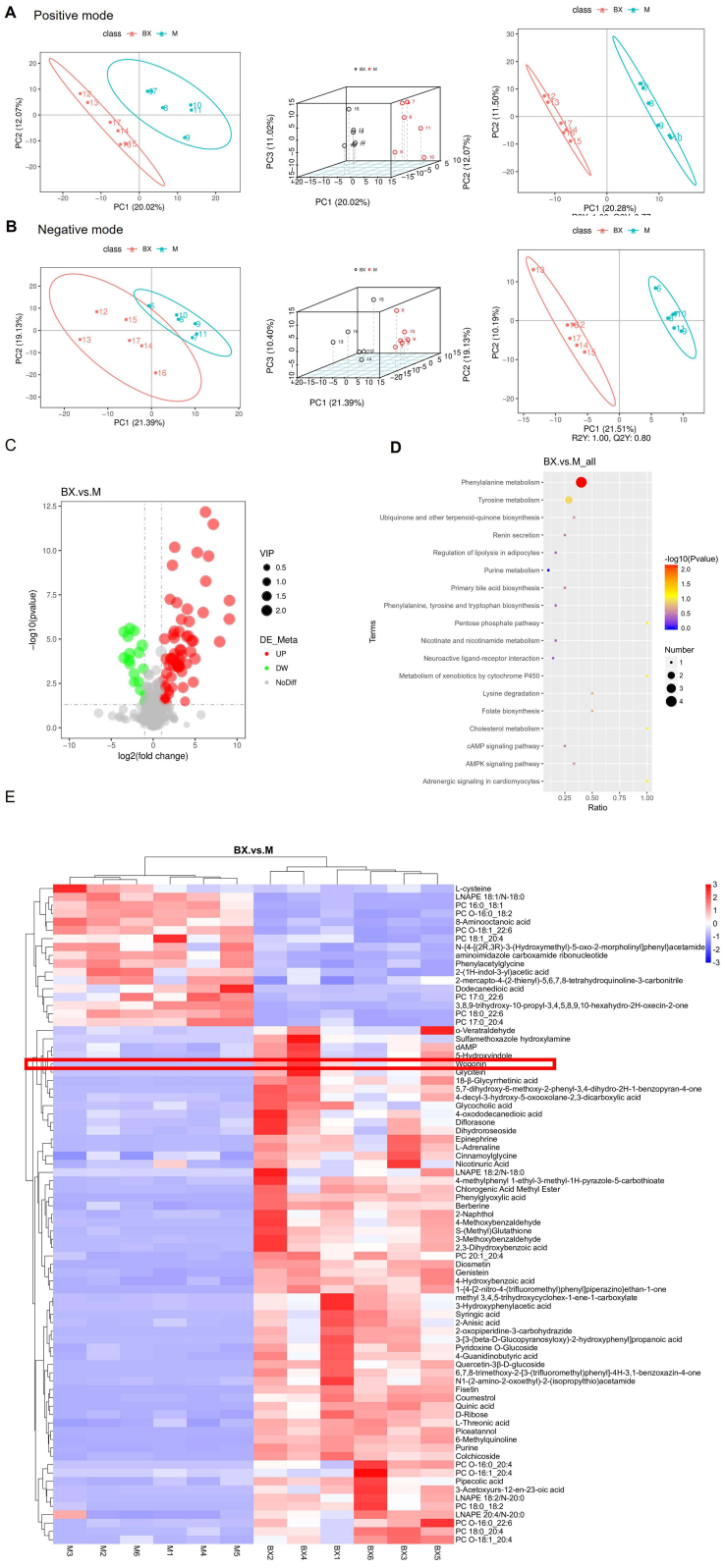

Figure 7 Metabolite changes in APP/PS1 double transgenic mice following the BXD intervention. (**A**) PCA, PCA 3D, PLSDA plots of serum samples in the positive modes. (**B**) PCA, PCA 3D, PLSDA plots of serum samples in the negative modes. (**C**) Metabolomics heat map. (**D**) Metabolic pathways of differential metabolites. (E) Major differential metabolites.

https://doi.org/10.2147/DDDT.S499852

neurons and glial cells, triggering inflammatory responses and contributing to neuronal damage.[34] Targeting the AGE-RAGE pathway can help reduce neuroinflammation and oxidative stress, thereby slowing the progression of AD. This pathway is particularly relevant given the increasing evidence linking metabolic dysregulation and chronic inflammation to AD pathology.[35] IL-17 is a pro-inflammatory cytokine that plays a significant role in the immune response and has been implicated in neuroinflammation. Elevated levels of IL-17 have been observed in the brains of AD patients, suggesting its involvement in the disease process.[36] IL-17 can promote the activation of microglia and astrocytes, leading to the release of other pro-inflammatory cytokines and contributing to neuronal damage. Modulating the IL-17 pathway can potentially reduce neuroinflammation and mitigate the inflammatory cascade in AD.[37] Given the prominent position of the PI3K/Akt signaling pathway in KEGG analyses and its regulatory influence on apoptosis and inflammation, this study posits that the PI3K/Akt signaling pathway may exert a significant role in the anti-AD effects of BXD.[38] The verification outcomes highlighted a pronounced inactivity within the PI3K/Akt pathway among $A\beta_{42}$-stimulated SY5Y cells, with BXD mitigating this reduction, suggesting its therapeutic efficacy in combating AD. However, the causal relationship between the PI3K/Akt pathway and BXD in the cellular and behavioral regulation of AD requires further investigation. NF-κB is a downstream component of the PI3K/Akt signaling pathway. Its activation is mediated through the phosphorylation of IκB kinase (IKK), which subsequently leads to the degradation of IκB13. The PI3K/Akt signaling pathway is a member of the serine/threonine kinase-related signaling family and has the capacity to modulate the NF-κB signaling pathway through the phosphorylation of p65 and IκBα. Furthermore, the findings unveiled that the NF-κB signaling pathway functions downstream of the PI3K/AKT signaling pathway during inflammatory processes.

Neuroinflammation is recognized as one of the core pathologies of AD and is characterized by a complex immune response of the central nervous system resulting in inflammatory cell infiltration, glial cell formation, and neuron loss.[39] This process is marked by the production of pro-inflammatory cytokines, including TNF-α, IL-6, and IL-1β, which causes proteins to misfold and cluster in neurons or intercellular neurons, forming neurofibrillary tangles and age spots in the cerebral cortex and hippocampus.[40] As AD progresses, levels of IL-6 may potentially increase, which could be associated with inflammatory responses in the brain. Furthermore, IL-6 may correlate with cognitive decline and brain atrophy in AD patients. In AD mouse models, blocking IL-6 signaling can reduce the decline in cognitive flexibility and the load of amyloid plaques.[41] Activation of the NLRP3 inflammasome has been documented both in the brain and peripherally in individuals presenting with AD pathology. Moreover, monocytes derived from AD patients exhibit an augmented production of caspase-1 and IL-1β in response to NLRP3 activation.[42] Moreover, apoptosis has been shown to be a key factor in neurodegeneration and therapy for AD.[43] Aβ peptides, which are a primary component of amyloid plaques in AD, can induce apoptosis in neurons. Aβ oligomers and fibrils can activate cell death pathways, leading to increased neuronal apoptosis and further exacerbating neuronal loss.[44] Literature indicates that the age-related alterations in Bcl-2 expression within the healthy brain parenchyma are distinct from the patterns observed in AD models. Specifically, Bcl-2 exhibits a downregulation in the neuronal populations of the AD-affected.[45] First at the vitro experimental level, we measured the expression levels of key inflammatory markers (IL-6, IL-1β, TNF-α, NF-κB, NLRP3, ASC, Caspase-1, pro-IL1β) using ELISA and WB. BXD treatment significantly reduced the levels of these markers compared to controls. We used flow cytometry with Annexin V-FITC and propidium iodide (PI) staining to quantify apoptosis. BXD treatment decreased the percentage of apoptotic cells, indicating its anti-apoptotic effects. Then at the vivo experimental level, we used APP/PS1 mice to assess the effects of BXD in vivo. Mice were treated with BXD for 4 months, and control groups received vehicle treatment. We conducted behavioral tests, including the Y-maze and new object recognition experiment, to evaluate cognitive function. BXD-treated mice showed significant improvements in cognitive performance compared to controls. We used RT-qPCR to detect apoptosis-related markers (Bax, Bcl-2, caspase 3) and inflammatory markers (IL-1β, TNF-α, NF-κB). BXD improved the expression of these markers in APP/PS1 mice. In the context of this study, the in vivo model utilized was the well-recognized APP/PS1 transgenic mouse model for AD. For the in vitro model, we employed SH-SY5Y cells induced by Aβ42. Consequently, this study was designed to elucidate the mechanisms by which BXD exerts its anti-AD effects, with a particular focus on the interplay between neuroinflammation and apoptosis. However, we posit that the composition of BXD encompasses ingredients with heat-clearing and detoxifying properties. Therefore, we speculate that BXD may also exert beneficial effects in other neuroinflammatory conditions.

The current behavioral assays utilized to assess the cognitive and mnemonic functions in murine models of AD include a range of well-established tests, such as the Morris water maze, Y-maze, novel object recognition task, open field test, light-dark box exploration, and the elevated plus maze.[46] The Morris water maze was implemented to evaluate spatial reference memory and working memory in AD animal models. The Y-maze was used to probe spatial short-term memory in these animals. The novel object recognition task assessed recognition memory in AD mice. Additionally, the open field test, light-dark box test, and elevated plus maze were employed to examine affective behaviors and anxiety-related responses in AD mice.[47] These extensive behavioral assessments are crucial for characterizing the neurocognitive and emotional profiles of the animals. In this experiment, Y-maze results showed that BXD improved the short-term memory ability of APP/PS1 mice。The results of the new object recognition experiment showed that BXD improved both long-term and short-term memory in APP/PS1 mice.

The metabolomics approach can provide minute details of biological pathways or mutations and is a powerful technique for identifying substances that contribute to brain function maintenance.[48] Numerous metabolomic changes have been identified after BXD administration in AD mice. Phenylalanine is an essential amino acid that plays a crucial role in protein synthesis and neurotransmitter production. In AD, alterations in phenylalanine metabolism may contribute to oxidative stress and neuroinflammation, as phenylalanine is a precursor for the synthesis of catecholamines, which can generate reactive oxygen species (ROS) upon metabolism.[49,50] Our metabolomic analysis revealed a significant decrease in phenylalanine levels in BXD-treated samples compared to controls. This reduction suggests that BXD may modulate phenylalanine metabolism, potentially reducing oxidative stress and neuroinflammation. By lowering phenylalanine levels, BXD may help mitigate the oxidative burden on neurons, thereby contributing to its neuroprotective effects. Pantothenic acid is a precursor for the synthesis of coenzyme A (CoA), which is essential for various metabolic processes, including fatty acid synthesis and energy production.[51] In AD, disturbances in energy metabolism and mitochondrial function are common, and pantothenic acid plays a critical role in maintaining cellular energy homeostasis.[52] The metabolomic data showed an increase in pantothenic acid levels following BXD treatment. This elevation indicates that BXD may enhance the availability of pantothenic acid, thereby supporting mitochondrial function and energy metabolism. Improved energy production is crucial for maintaining neuronal health and function, which is often compromised in AD. By increasing pantothenic acid levels, BXD may help restore metabolic balance and support neuronal resilience against AD pathology. More importantly, we preliminarily screened out the main active components of BXD through metabolomics and network pharmacology. Baicalein, Wogonin, and Oroxylin A has been reported to exhibit protective effects against AD by inhibiting the amyloidogenic pathway.[53,54] Our findings on the therapeutic potential of BXD for AD are interpreted within the broader context of traditional herbal formulations. BXD, like other TCM formulations, is characterized by its multi-component nature, which allows for a holistic approach to treating complex diseases such as AD. The identified active components, including wogonin, are part of a synergistic network that targets multiple pathways implicated in AD pathology. This multi-target approach is consistent with the principles of TCM, which emphasizes the balance and interaction of various herbal components to achieve therapeutic effects. Several studies have employed network pharmacology and metabolomics to explore the therapeutic mechanisms of traditional herbal formulations.[14,55–58] Unlike them, in this study, network pharmacology, metabolomics and UHPLC-QE-MS analysis jointly screened out the common component Wogonin as a possible main component of BXD anti-AD. Integrating the results from network pharmacology screening, we identified several key components in BXD, including Stigmasterol, Acacetin, Nuciferin, Wogonin, Baicalein, and Oroxylin A, which were detected in the drug-containing serum. Subsequently, we cross-referenced these components with the metabolomics data and determined that Wogonin is the compound jointly identified by network pharmacology, UHPLC-QE-MS, and metabolomics. Based on these findings, we hypothesize that Wogonin may be a principal component of BXD responsible for its therapeutic effects on AD.

In comparison to conventional AD treatments, BXD, a traditional Chinese medicine, boasts the benefits of multi-target efficacy, proven safety, and minimal side effects.[59–64] Our team has conducted a comprehensive exploration of the mechanisms underlying the prevention and treatment of AD with BXD. Previous studies published by us have demonstrated that BXD can improve cerebral glucose metabolism, which is crucial in the management of AD. We have also explored the optimal dosage for BXD's therapeutic effects on AD and found that a moderate dose to be the most effective.[65] Consequently, this study continues to employ this effective dosage for further investigation. In contrast

to our previous studies, this research utilizes network pharmacology to identify targets and active ingredients. Based on our earlier work, we have conducted further investigations into the mechanisms of BXD and discovered that neuroinflammation and apoptosis may be the primary key mechanisms through which BXD ameliorates AD.

Current treatments for AD primarily focus on symptom management and include cholinesterase inhibitors (eg, donepezil, rivastigmine) and NMDA receptor antagonists (eg, memantine). These medications provide modest improvements in cognitive function but do not fundamentally alter the disease course. BXD represents a promising complementary approach within the broader landscape of AD treatment. BXD's multi-target efficacy, rooted in TCM, offers a holistic strategy that addresses multiple pathological pathways implicated in AD, such as neuroinflammation, oxidative stress, and mitochondrial dysfunction. BXD's ability to modulate these pathways suggests it could provide synergistic benefits when used in combination with existing therapies, potentially enhancing overall treatment efficacy and improving patient outcomes. Ensuring that the active components of BXD reach therapeutic concentrations in the brain is a significant challenge. The blood-brain barrier (BBB) can limit the entry of many compounds, necessitating strategies to enhance bioavailability. Future research should explore formulations that improve the permeability of BXD's active ingredients across the BBB. This could include nanoparticle delivery systems, prodrug strategies, or the use of permeation enhancers. Then, standardizing the dosage of BXD to ensure consistent therapeutic outcomes is crucial. Variations in the potency of herbal ingredients can affect the efficacy and safety of the formulation. Rigorous quality control measures, including standardized extraction methods and the use of validated markers for potency, are essential. Collaborative efforts with regulatory bodies to establish guidelines for dosage standardization will be necessary. Our next step in clinical trials will be to evaluate the safety, tolerability and pharmacokinetics of BXD in healthy volunteers and patients with early-stage AD. Randomized, double-blind, placebo-controlled trial with multiple ascending doses (MAD) and single ascending doses (SAD) to determine the optimal dosing regimen and identify any adverse effects.

Conclusions

In the study, we employed a multifaceted approach encompassing network pharmacology, metabolomics, and UHPLC-QE-MS detection to elucidate the potential targets and molecular mechanisms underlying the anti-AD effects of BXD. Our experimental findings have revealed that BXD exerts significant therapeutic effects by modulating neuroinflammation, apoptosis, and the PI3K/Akt signaling pathway, thereby mitigating learning, memory, and cognitive deficits associated with AD. This study demonstrates that BXD's multi-target effects address critical AD pathologies, providing a strong foundation for its development as a complementary therapeutic strategy. The mechanism diagram is shown in Figure 8.

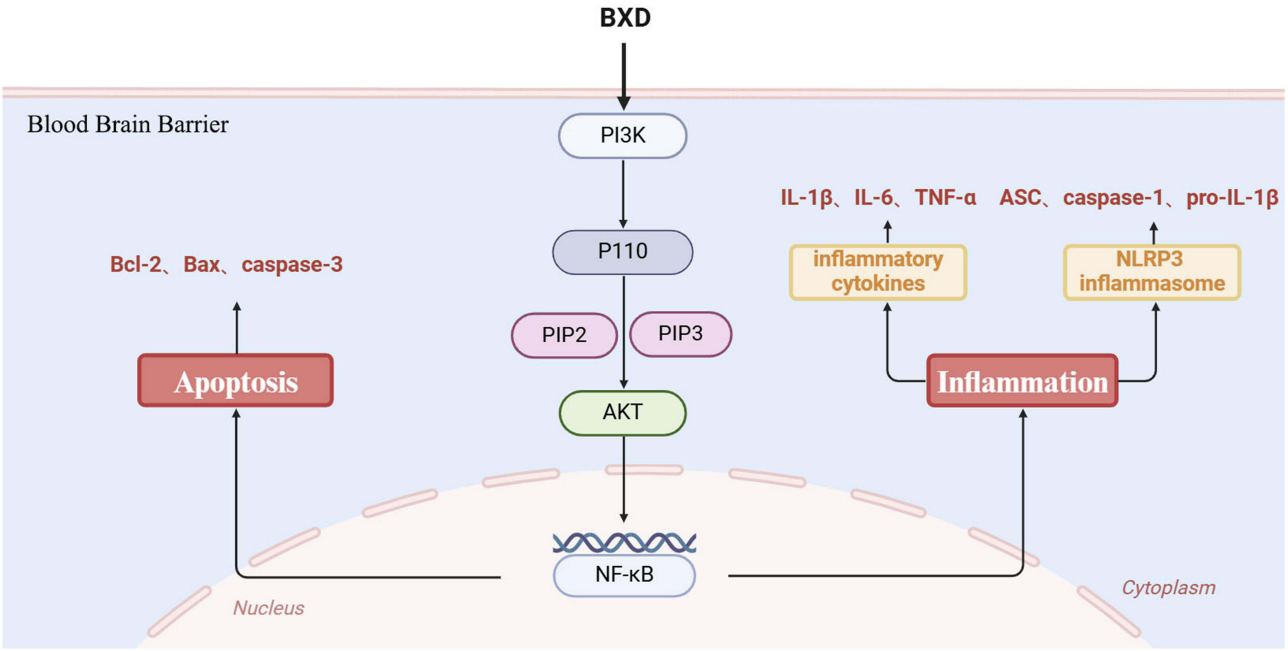

Figure 8 BXD improves AD mechanism simulation diagram.

Abbreviations

AD, Alzheimer's disease; Aβ, Beta-amyloid; RT-qPCR, Reverse transcription quantitative real-time polymerase chain reaction; IL-6, Interleukin-6; IL-1β, Interleukin-1β; NF-κB, Nuclear factor kappa-B; Akt, Protein kinase B; CNS, Central nervous system; PI3K, Phosphoinositide 3-kinase; TNF-α, Tumor necrosis factor-α; NFTs, Neurofibrillary tangles.

Data Sharing Statement

The datasets used and/or analyzed during the current study are available from the corresponding author upon reasonable request.

Ethics Statement

All processes involving mice were authorized by the Binzhou Medical University Hospital's Animal Ethics and Welfare Committee granted approved the experimental procedures; 20230206-64 was the approval number for this process.

Funding

This study was supported by Natural Science Foundation of Shandong Province (ZR2023QH030, ZR2024MH089 to QGF, ZR2022YQ65 to CL, ZR2021MH073 to CL), the National Natural Science Foundation of China (82171521, 82371539 to CL), Special Funds of the Taishan Scholars Project of Shandong Province (No. tsqn202211368 to CL), the Projects of Traditional Chinese medicine in Shandong Province (Z20244105to RQS; Q-2023005 to FTM; M-2023120 to DW), the Scientific Research Foundation of Binzhou Medical University (BY2021KYQD31).

Disclosure

Gaofeng Qin and Rongqiang Song are joint first authors. The authors report no conflicts of interest in this work.

References

1. Scheltens P. et al. Alzheimer's disease. *Lancet*. 2021;24.
2. Luo YX, Yang LL, Yao XA-O. Gut microbiota-host lipid crosstalk in Alzheimer's disease: implications for disease progression and therapeutics. *Mol Neurodegener*. 2024;19(1):35. doi:10.1186/s13024-024-00720-0
3. Wang GQJ, Liu X, Miller G, Vardarajan B, Baccarelli A, Guo Z. Alzheimer's disease report in China 2024. *Diagnostics Theory and Pract*. 2024;23 (03):219–256.
4. Steel K. Alzheimer's disease. *N Engl J Med*. 2010;362(19):1844. author reply 1844-5.
5. Rostagno AA. Pathogenesis of Alzheimer's Disease. *Int J mol Sci*. 2022;24(1):107–125. doi:10.3390/ijms24010107
6. Beata BK, Wojciech J, Johannes K, et al. Alzheimer's disease-biochemical and psychological background for diagnosis and treatment. *Int J mol Sci*. 2023;24(2):1059–1072. doi:10.3390/ijms24021059
7. Jiang Y, Gao H, Turdu G. Traditional Chinese medicinal herbs as potential AChE inhibitors for anti-Alzheimer's disease: a review. *Bioorg Chem*. 2017;75:50–61. doi:10.1016/j.bioorg.2017.09.004
8. Shi Y, et al. Banxia xiexin decoction prevents HT22 cells from high glucose-induced neurotoxicity via JNK/SIRT1/Foxo3a signaling pathway. *Curr Comput Aided Drug Des*. 2023;4(22):1–17.
9. Chen F, He Y, Wang P, et al. Banxia Xiexin decoction ameliorated cognition via the regulation of insulin pathways and glucose transporters in the hippocampus of APPswe/PS1dE9 mice. *Int J Immunopathol Pharmacol*. 2018;32:2058738418780066. doi:10.1177/2058738418780066
10. Lanznaster D, Mack JM, Coelho V, et al. Guanosine prevents anhedonic-like behavior and impairment in hippocampal glutamate transport following amyloid-β(1-40) administration in mice. *mol Neurobiol*. 2017;7(54):5482–5496. doi:10.1007/s12035-016-0082-1
11. Cui J, Wang J, Zheng M, et al. Ginsenoside Rg2 protects PC12 cells against β-amyloid(25-35)-induced apoptosis via the phosphoinositide 3-kinase/ Akt pathway. *Chem Biol Interact*. 2017;25(1872–7786):152–161. doi:10.1016/j.cbi.2017.07.021
12. Li X, Chen J, Feng W, et al. Berberine ameliorates iron levels and ferroptosis in the brain of 3 × Tg-AD mice. *Phytomedicine*. 2023;9(118):1–15.
13. Huang X, Wang Y, Ren K. Protective effects of liquiritin on the brain of rats with Alzheimer's disease. *West Indian Med J*. 2015;64(5):468–472. doi:10.7727/wimj.2016.058
14. Li Q, Jia C, Wu H, et al. Nao Tan Qing ameliorates Alzheimer's disease-like pathology by regulating glycolipid metabolism and neuroinflammation: a network pharmacology analysis and biological validation. *Pharmacol Res*. 2022;11(10):106489. doi:10.1016/j.phrs.2022.106489
15. Zhi J, Yin L, Zhang Z, et al. Network pharmacology-based analysis of Jin-Si-Wei on the treatment of Alzheimer's disease. *J Ethnopharmacol*. 2024;30(18):117291. doi:10.1016/j.jep.2023.117291
16. Wu Q, Wang W, Huang Z, et al. Unveiling the molecular mechanisms of Danggui-Shaoyao-San against Alzheimer's disease in APP/PS1 mice via integrating proteomic and metabolomic approaches. *Alzheimers Res Ther*. 2024;16(1):251. doi:10.1186/s13195-024-01618-1
17. Yi L, Liu W, Wang Z, et al. Characterizing Alzheimer's disease through metabolomics and investigating anti-Alzheimer's disease effects of natural products. *Ann N Y Acad Sci*. 2017;13(1):130–141. doi:10.1111/nyas.13385

18. Zhang M, Niu H, Li Q, et al. Active compounds of panax ginseng in the Improvement of Alzheimer's disease and application of spatial metabolomics. LID - 10.3390/ph17010038 [doi] LID - 38. *Pharmaceuticals (Basel)*. 2023;17(1):38. doi:10.3390/ph17010038
19. Park MW, Cha HW, Kim J, et al. NOX4 promotes ferroptosis of astrocytes by oxidative stress-induced lipid peroxidation via the impairment of mitochondrial metabolism in Alzheimer's diseases. *Redox Biol*. 2021;41(1):101947. doi:10.1016/j.redox.2021.101947
20. Fu X, Liu J, Xie J, et al. Identification of potential therapeutic and diagnostic characteristics of Alzheimer disease by targeting the miR-132-3p/FOXO3a-PPM1F axis in APP/PS1 mice. *Brain Res*. 2022;1790:147983. doi:10.1016/j.brainres.2022.147983
21. Qin G, Dong Y, Liu Z, et al. Shen-Zhi-Ling oral liquid ameliorates cerebral glucose metabolism disorder in early AD via insulin signal transduction pathway in vivo and in vitro. *Chin Med*. 2021;16(1):128. doi:10.1186/s13020-021-00540-0
22. Ma X, Li Q, Chen G, et al. Role of Hippocampal miR-132-3p in modifying the function of protein phosphatase Mg2+/Mn2+-dependent 1 F in depression. *Neurochem Res*. 2023;48(8):2514–2530. doi:10.1007/s11064-023-03926-8
23. Sun Z, Wang M, Xu L, et al. PPARgamma/Adiponectin axis attenuates methamphetamine-induced conditional place preference via the hippocampal AdipoR1 signaling pathway. *Prog Neuropsychopharmacol Biol Psychiatry*. 2023;125:110758. doi:10.1016/j.pnpbp.2023.110758
24. Akyol S, Ugur Z, Yilmaz A, et al. Lipid profiling of Alzheimer's disease brain highlights enrichment in glycerol(phospho)lipid, and sphingolipid metabolism. *Cells*. 2021;10(10):2591–2602. doi:10.3390/cells10102591
25. Wei W, Norton DD, Wang X, Kusiak JW, et al.. Abeta 17-42 in Alzheimer's disease activates JNK and caspase-8 leading to neuronal apoptosis. *Brain*. 2002;125(Pt 9):2036–2043. doi:10.1093/brain/awf205
26. Heneka MT, Kummer MP, Stutz A, et al. NLRP3 is activated in Alzheimer's disease and contributes to pathology in APP/PS1 mice. *Nature*. 2013;493(7):674–678. doi:10.1038/nature11729
27. Gong D, Yuan T, Wang R, et al. Network pharmacology approach and experimental verification of Dan-Shen decoction in the treatment of ischemic heart disease. *Pharm Biol*. 2023;61(1):69–79. doi:10.1080/13880209.2022.2152059
28. Kumar M, Bansal N. Implications of phosphoinositide 3-kinase-Akt (PI3K-Akt) pathway in the pathogenesis of Alzheimer's disease. *mol Neurobiol*. 2022;59(1):354–385.
29. Gao WY, Tian M-Y, Li M-L, et al. Study on the potential mechanism of Qingxin Lianzi Yin Decoction on renoprotection in db/db mice via network pharmacology and metabolomics. *Phytomedicine*. 2023;126(126):155222. doi:10.1016/j.phymed.2023.155222
30. He D, Huang J-H, Zhang Z-Y, et al. A network pharmacology-based strategy for predicting active ingredients and potential targets of liuwei dihuang pill in treating type 2 diabetes mellitus. *Drug Des Devel Ther*. 2019;13(13):3989–4005. doi:10.2147/DDDT.S216644
31. Han X, Bao J, Ni J, et al. Qing Xia Jie Yi Formula (QXJYF) granules alleviated acute pancreatitis through inhibition of M1 macrophage polarization by suppressing glycolysis. *J Ethnopharmacol*. 2024;10(18):1–43.
32. Kumar MA-OX, Bansal NA-O. Implications of Phosphoinositide 3-Kinase-Akt (PI3K-Akt) pathway in the pathogenesis of Alzheimer's disease. *mol Neurobiol*. 2022;59(1):354–385. doi:10.1007/s12035-021-02611-7
33. Khezri MR, Esmaeili A, Ghasemnejad-Berenji M. Platelet activation and Alzheimer's disease: the probable role of PI3K/AKT pathway. *J Alzheimers dis*. 2022;90(2):529–534. doi:10.3233/JAD-220663
34. Wang YY, Zhou Y-N, Jiang L, et al. Long-term voluntary exercise inhibited AGE/RAGE and microglial activation and reduced the loss of dendritic spines in the hippocampi of APP/PS1 transgenic mice. *Exp Neurol*. 2023;5(363):114371. doi:10.1016/j.expneurol.2023.114371
35. Maczurek AG, Shanmugam KF, Münch G, u - Münch, and G.Münch. Inflammation and the redox-sensitive AGE-RAGE pathway as a therapeutic target in Alzheimer's disease. *Ann N Y Acad Sci*. 2008;4(11):147–151. doi:10.1196/annals.1433.026
36. Maczurek AG, Shanmugam KF, Tomic I, u Münch, and G. Münch. Inflammation and the redox-sensitive AGE-RAGE pathway as a therapeutic target in Alzheimer's disease. *Gut Microbes*. 2024;16(1):2363014. doi:10.1080/19490976.2024.2363014
37. Yang J, Kou J, Lalonde R, et al. Intracranial IL-17A overexpression decreases cerebral amyloid angiopathy by upregulation of ABCA1 in an animal model of Alzheimer's disease. *Brain Behav Immun*. 2017;10(65):262–273. doi:10.1016/j.bbi.2017.05.012
38. Ding MR, Qu Y-J, Hu B, et al. Signal pathways in the treatment of Alzheimer's disease with traditional Chinese medicine. *Biomed Pharmacother*. 2022;152(1):113208. doi:10.1016/j.biopha.2022.113208
39. Rodríguez Murúa S, Farez MF, Quintana FJ. The immune response in multiple sclerosis. *Annu Rev Pathol*. 2022;17(24):121–139. doi:10.1146/annurev-pathol-052920-040318
40. Chen Y, Peng F, Xing Z, Chen J, Peng C, Li D. Beneficial effects of natural flavonoids on neuroinflammation. *Front Immunol*. 2022;24(13):1–16.
41. Kang S, Narazaki M, Metwally H, et al. Historical overview of the interleukin-6 family cytokine. LID - 10.1084/jem.20190347 [doi] LID - e20190347. *J Exp Med*. 2020;217(5):e20190347. doi:10.1084/jem.20190347
42. McManus RM, Latz E. NLRP3 inflammasome signalling in Alzheimer's disease. *Neuropharmacology*. 2024;1(2):109941. doi:10.1016/j.neuropharm.2024.109941
43. Obulesu M, Lakshmi MJ. Apoptosis in Alzheimer's disease: an understanding of the physiology, pathology and therapeutic avenues. *Neurochem Res*. 2014;39(12):2301–2312. doi:10.1007/s11064-014-1454-4
44. Shimohama S. Apoptosis in Alzheimer's disease–an update. *Apoptosis*. 2000;5(1):9–16. doi:10.1023/A:1009625323388
45. Callens M, Kraskovskaya N, Derevtsova K, et al. The role of Bcl-2 proteins in modulating neuronal Ca(2+) signaling in health and in Alzheimer's disease. *Biochim Biophys Acta mol Cell Res*. 2021;5(6):118997. doi:10.1016/j.bbamcr.2021.118997
46. Sun XY, Li L-J, Dong Q-X, et al. Rutin prevents tau pathology and neuroinflammation in a mouse model of Alzheimer's disease. *J Neuroinflammation*. 2021;18(1):131. doi:10.1186/s12974-021-02182-3
47. Zhou XL, Xu M-B, Jin T-Y, et al. Preclinical evidence and possible mechanisms of extracts or compounds from cistanches for Alzheimer's disease. *Aging Disease*. 2019;10(5):1075–1093. doi:10.14336/AD.2018.0815-1
48. Botello Marabotto M, Martínez-Bisbal MC, Calero M, et al. Non-invasive biomarkers for mild cognitive impairment and Alzheimer's disease. *Neurobiol Disease*. 2023;10(15):1–13.
49. Spoleti E, La Barbera L, Cauzzi E, et al. Dopamine neuron degeneration in the ventral tegmental area causes hippocampal hyperexcitability in experimental Alzheimer's Disease. *mol Psychiatry*. 2024;29(5):1265–1280. doi:10.1038/s41380-024-02408-9
50. Ambeskovic M, Hopkins G, Hoover T, et al. Metabolomic signatures of Alzheimer's disease indicate brain region-specific neurodegenerative progression. LID - 10.3390/ijms241914769 [doi] LID - 14769. *Int J mol Sci*. 2023;24(19):14769. doi:10.3390/ijms241914769

51. Xu J, Patassini S, Begley P, et al. Cerebral deficiency of vitamin B5 (d-pantothenic acid; pantothenate) as a potentially-reversible cause of neurodegeneration and dementia in sporadic Alzheimer's disease. *Biochem Biophys Res Commun*. 2020;527(3):676–681. doi:10.1016/j.bbrc.2020.05.015
52. Scholefield M, Church SJ, Xu J, et al. Localized Pantothenic Acid (Vitamin B5) Reductions Present Throughout the Dementia with Lewy Bodies Brain. *J Parkinsons Dis*. 2024;14(5):965–976. doi:10.3233/JPD-240075
53. Huang DS, Yu Y-C, Wu C-H, et al. Protective effects of wogonin against alzheimer's disease by inhibition of amyloidogenic pathway. *Evid Based Complement Alternat Med*. 2017;6(7):3545169. doi:10.1155/2017/3545169
54. Ji Y, Han J, Lee N, et al. Neuroprotective effects of baicalein, wogonin, and oroxylin a on amyloid beta-induced toxicity via NF-κB/MAPK Pathway Modulation. LID - 10.3390/molecules25215087 [doi] LID - 5087. *Molecules*. 2020;25(21):5087. doi:10.3390/molecules25215087
55. Liu Y, Li H, Wang X, et al. Anti-Alzheimers molecular mechanism of icariin: insights from gut microbiota, metabolomics, and network pharmacology. *J Transl Med*. 2023;21(1):277. doi:10.1186/s12967-023-04137-z
56. Zhang Z, Yi P, Yang J, et al. Integrated network pharmacology analysis and serum metabolomics to reveal the cognitive improvement effect of Bushen Tiansui formula on Alzheimer's disease. *J Ethnopharmacol*. 2020;1(1):112371. doi:10.1016/j.jep.2019.112371
57. Fan Y, Wang A, Liu Z, et al. Integrated spatial metabolomics and network pharmacology to explore the pharmacodynamic substances and mechanism of Radix ginseng-Schisandra chinensis Herb Couple on Alzheimer's disease. *Anal Bioanal Chem*. 2024;416(19):4275–4288. doi:10.1007/s00216-024-05364-z
58. Wang F, Chen H, Hu Y, et al. Integrated comparative metabolomics and network pharmacology approach to uncover the key active ingredients of Polygonati rhizoma and their therapeutic potential for the treatment of Alzheimer's disease. *Front Pharmacol*. 2022;4(13):934947. doi:10.3389/fphar.2022.934947
59. Ramakrishna KA-O, Karuturi P, Siakabinga Q, et al. Indole-3 carbinol and diindolylmethane mitigated β-amyloid-induced neurotoxicity and acetylcholinesterase enzyme activity. *Silico, in Vitro, and Network Pharmacology Study Diseases*. 2024;12(8):184.
60. Tripathi PN, Lodhi A, Rai SN, et al. Review of pharmacotherapeutic targets in Alzheimer's disease and its management using traditional medicinal plants. *Degener Neurol Neuromuscul Dis*. 2024;19(14):47–74.
61. Singh MA-O, Agarwal V, Pancham P, et al. A comprehensive review and androgen deprivation therapy and its impact on Alzheimer's disease risk in older men with prostate cancer. *Degener Neurol Neuromuscul Dis*. 2024;5(17):33–46.
62. Tripathi PN, Srivastava P, Sharma P, et al. Biphenyl-3-oxo-1,2,4-triazine linked piperazine derivatives as potential cholinesterase inhibitors with anti-oxidant property to improve the learning and memory. *Bioorg Chem*. 2019;4(85):82–96. doi:10.1016/j.bioorg.2018.12.017
63. Srivastava P, Tripathi PN, Sharma P, et al. Design and development of some phenyl benzoxazole derivatives as a potent acetylcholinesterase inhibitor with antioxidant property to enhance learning and memory. *Eur J Med Chem*. 2019;163(4):116–135. doi:10.1016/j.ejmech.2018.11.049
64. Rai SN, Singh C, Singh A, et al. Mitochondrial dysfunction: a potential therapeutic target to treat Alzheimer's disease. *mol Neurobiol*. 2020;57(7):3075–3088. doi:10.1007/s12035-020-01945-y
65. Gao CY, Qin GF, Zheng MC, Tian MJ, He YN, Wang PW. Banxia xiexin decoction alleviated cerebral glucose metabolism disorder by regulating intestinal microbiota in APP/PS1 Mice.*Chin J Integr Med*. 2024;21(2):1–10.